Effects of various polycyclic aromatic hydrocarbons on cell signaling pathways with a particular focus on inflammation

Aurora Dorothea Lauritsen

Master of Toxicology and Environmental Sciences

Department of Biosciences

Faculty of Mathematics and Natural Sciences

UNIVERSITY OF OSLO

2020

2020

Title: Effects of various polycyclic aromatic hydrocarbons on cell signaling pathways with a particular focus on inflammation

Author: Aurora Dorothea Lauritsen

http://www.duo.uio.no

Print: Reprosentralen, Universitetet i Oslo

Acknowledgments

This thesis was performed at the Norwegian Institute of Public Health (NIPH), at the Department of Air pollution and Noise. I was supervised by Dr. Jørn A. Holme and Co-supervisor Dr. Johan Øvrevik.

I would like to thank my supervisors for this opportunity, and especially Jørn, for the tremendous support during the writing and all the educational and interesting conversations. Secondly, I would like to thank Johan for making time in his busy schedule, and for his immense support when it has been most needed. A special thanks to Tonje Scwhach Skuland for teaching me the laboratory techniques, answering my questions, and for the friendly conversations. I also want to thank Vegard Sæter Grytting for the entertaining chats, constructive criticism, and for sharing his knowledge. Also, a special thank you to all the other people in the department who have been very kind, supportive, and for sharing their knowledge with me. I also want to thank the department director, Christine Instanes, for her understanding and flexibility during difficult times, making it possible for me to finish my laboratory work in time.

Also, a special thanks to family and friends who have supported me during this extraordinary and challenging period during the pandemic. Thank you, mom, for your understanding and for motivating and helping me to follow my dreams. Lastly, to my boyfriend, Zvonimir Grubišić, thank you for the motivation, good conversations, laughter, and for all the love and care you have given me. Thank you for supporting and believing in me.

Oslo, September 2020

Aurora Dorothea Lauritsen

Abstract

Polycyclic aromatic hydrocarbons (PAHs) are a group of chemical compounds found in urbane air, which have been suggested to contribute to pulmonary diseases by modulating pro-inflammatory responses. The relative potency of the various PAHs and signaling pathways behind the PAH-induced inflammation are not well known. Therefore, we wanted to assess if various PAHs modulates the aryl hydrocarbon receptor (AhR) and the possible importance of AhR in altering pro-inflammatory responses. We exposed human bronchial epithelial cells (BEAS-2B) to eight different PAHs; phenanthrene, 1-methylphenanthrene (1-MP), fluoranthene, pyrene, 1-nitropyrene (1-NP), β-naphthoflavone (β-NF), benzo[*a*]pyrene (B[*a*]P), and benzo[*e*]pyrene (B[*e*]P). All the PAHs modulated AhR through altering *CYP1A1* expression. B[*a*]P, B[*e*]P, and phenanthrene had agonistic properties towards AhR, whereas the other PAHs (1-MP, fluoranthene, pyrene, and 1-NP) had antagonistic properties. Notably, the agonistic/antagonistic abilities seemed to be partly concentration-dependent. The tested PAHs generally had none or marginal effects on the IL-6 release. In contrast, they did not markedly change the CXCL8 release. When the cells were primed with the Toll-like receptor 3 (TLR3) agonist polyinosinic:polycytidylic (Poly I:C), which mimics a viral infection, pyrene slightly increased the IL-6 and CXCL8 release, but the other PAHs did not cause any marked changes. However, there were some variations between the different experiments that may have masked the possible effects. Inhibiting AhR by treating the unprimed and primed cells with the AhR antagonist CH223191 illustrated that cytokine release in both unprimed and primed cells could be dependent on AhR activity. In contrast, inhibiting AhR caused no observable effect on *IL-6* and *CXCL8* expression in unprimed cells. Lastly, pyrene and B[*a*]P did not increase Ca^{2+} release as evaluated using Cal-520 AM dye and measuring fluorescence using a microplate fluorescence reader. However, it should be noted that the used method may not be sensitive enough to detect possible responses. This study elucidates that the PAHs may modulate the classical genomic pathway of AhR. However, using the present experimental model, their effects on pro-inflammatory responses seem to be marginal, were cytokine release appeared to be dependent on AhR activity, while the synthesis was unaffected.

Abbreviations

1-MP	1-Methylphenanthrene
1-NP	1-Nitropyrene
AhR	Aryl hydrocarbon receptor
ARNT	Aryl hydrocarbon receptor nuclear translocator
B[*a*]P	Benzo[*a*]Pyrene
B[*e*]P	Benzo[*e*]Pyrene
BEAS-2B	Bronchial epithelial cell line (Human SV40 transfected)
β-NF	β-naphthoflavone
$[Ca^{2+}]_i$	Intracellular calcium concentration
Ca^{2+}	Calcium ion
cDNA	Complementary DNA
CH223191	2-methyl-2H-pyrazole-3-carboxylic acid (2-methyl-4-o-tolylazo-phenyl)-amide
CO	Carbon monoxide
COPD	Chronic obstructive pulmonary disease
C_T	Cycle threshold value
CXCL8	Interleukin 8
CYP	Cytochrome P450
DMSO	Dimethyl sulfoxide
DNase	Deoxyribonuclease
DPM	Diesel particulate matter
dsRNA	Double-stranded RNA
ELISA	Enzyme-linked immunosorbent assay
GADPH	Glyceraldehyde-3-phosphate dehydrogenase
H_2O_2	Hydrogen peroxide
H_2SO_4	Sulfuric acid
HRP	Horseradish peroxidase
IL-6	Interleukin 6
INT	2-(4-iodophenyl)-3-(4-nitrophenyl)-5-phenyl-2H-tetrazolium
LDH	Lactate dehydrogenase
LPS	Lipopolysaccharide
mRNA	Messenger RNA
NCD	Non-communicable disease

NF-κB	Nuclear factor-κB
Nitro-PAHs	Nitrated polycyclic aromatic hydrocarbons
NO_x	Nitrogen oxides
$^{\bullet}OH$	Hydroxyl radical
$O_2^{\bullet -}$	Anion superoxide radical
O_3	Ozone
PAH	Polycyclic aromatic hydrocarbon
PAMPs	Pathogen-Associated Molecular Patterns
PM	Particulate matter
Poly I:C	Polyinosinic:polycytidylic acid
PRRs	Pattern Recognition Receptors
RNase	Ribonuclease
ROS	Reactive oxygen species
RT-qPCR	Quantitative reverse transcription polymerase chain reaction
SO_2	Sulfur dioxide
TCDD	2,3,7,8-tetrachlorodibenzodioxin
TLRs	Toll-Like Receptors
TMB	Tetramethyldbenzidine
UFPs	Ultrafine particles
XREs	Xenobiotic response elements

Table of Contents

1. Introduction

Air pollution and diesel particulate matter (DPM) has been associated with a higher risk of lung cancer in humans (IARC, 2014). The DPM contains polycyclic aromatic hydrocarbons (PAHs), which are known to be potent mutagens and carcinogens (IARC, 2010). Notably, earlier studies have increased the interest in the PAHs importance for inflammatory responses, and in the adverse health effect they may have for humans (IARC, 2010, 2014; Tokiwa, Sera, Horikawa, Nakanishi, & Shigematu, 1993).

1.1. Air pollution

Air pollution is a mixture of chemicals, gases, and biological material suspended in the air, which may cause harm to humans, animals, and vegetation (Kampa & Castanas, 2008). Air pollutants can be derived from the combustion of organic material from volcanoes and fires (Brunekreef & Holgate, 2002), including incomplete combustion of other organic materials, such as coal, fossil fuels and biomass (Landrigan et al., 2018). Some primary sources for emissions in newer times are various industrial activities, residential biomass burning, agricultural waste burning, and petroleum consumption by motor vehicles (Brunekreef & Holgate, 2002; Landrigan et al., 2018). The ambient air pollution is still increasing as a consequence of the industrialization of low-income countries and the rapid growth of cities, causing the increased usage of petroleum-fueled cars, buses, and trucks. Notably, the combustion of fuels has been reported to account for up to 85% of airborne particulate pollution (Landrigan et al., 2018). Thus, in newer times, we have been increasingly exposed to air pollution. However, legislation and regulations have recently been passed to prevent pollution, which has caused a reduction of the emissions in high- and middle-income countries (Landrigan et al., 2018), suggesting that the emission and our exposure to air pollution are slowly declining.

Many of the pollutants formed by combustion are lipophilic chemicals that potentially may accumulate in the body. Thus, long term exposure to natural sources has resulted in the evolutionary development of various defense mechanisms to protect us from the pollutants' harmful effects (Kampa & Castanas, 2008), including the development of xenobiotic-metabolizing enzymes. Furthermore, these enzymes may modify the lipophilic chemicals into water-soluble compounds, which the body readily excretes. Nevertheless, several pollutants may contribute to the development of various diseases. Epidemiological

studies suggest that air pollution and airborne particulate matter (PM) may harm human health, including being associated with increased occurrence of different cardiopulmonary conditions, chronic respiratory diseases, and lung cancers (Øvrevik et al., 2017).

1.2. Particulate matter (PM)

Combustion of organic matter will result in a mixture of PM, sulfur dioxide (SO_2), nitrogen oxides (NO_x), carbon monoxide (CO), and ozone (O_3) (Prüss-Ustün, Vickers, Haefliger, & Bertollini, 2011). PM is the term used for air pollutants that consist of different complex mixtures of particles suspended in the air (Kampa & Castanas, 2008). It contains a carbonaceous component and secondary components, including inorganic and organic chemicals, metals, and reactive gases (Kampa & Castanas, 2008; Schwarze et al., 2006). PM varies in size and composition and is categorized according to its aerodynamic equivalent diameter (size), as shown in Figure 1. Respirable particles also called thoracic particles, have a size ranging from 10 µm to 0.01 µm. Furthermore, they are characterized by the ability to pass the larynx and reach the primary bronchioles (Brook et al., 2004; Kelly & Fussell, 2012).

PM_{10} is defined as PM with a size of less than 10 µm. Coarse particles, which often include mineral particles, are designated $PM_{10-2.5}$ and range between 10 – 2.5 µm (Brook et al., 2004; Esworthy, 2013). These are large and often deposit in the throat and upper respiratory airways during inhalation, and are further eliminated by coughing or sneezing (Atkinson, Fuller, Anderson, Harrison, & Armstrong, 2010; Cadelis, Tourres, & Molinie, 2014). Fine particles ($PM_{2.5-0.1}$) range between 2.5 – 0.1 µm (Esworthy, 2013), and more strongly impact human health by being able to reach the alveoli and terminal bronchioles (Kelly & Fussell, 2012; Löndahl et al., 2007). Ultrafine particles (UFPs) have a size ranging between 0.1 – 0.01 µm and are designated $PM_{2.5}$ together with fine particles (Kelly & Fussell, 2012). UFPs have a higher surface area-to-mass ratio than the bigger particles, and may potentially lead to enhanced biological toxicity (Brook et al., 2004).

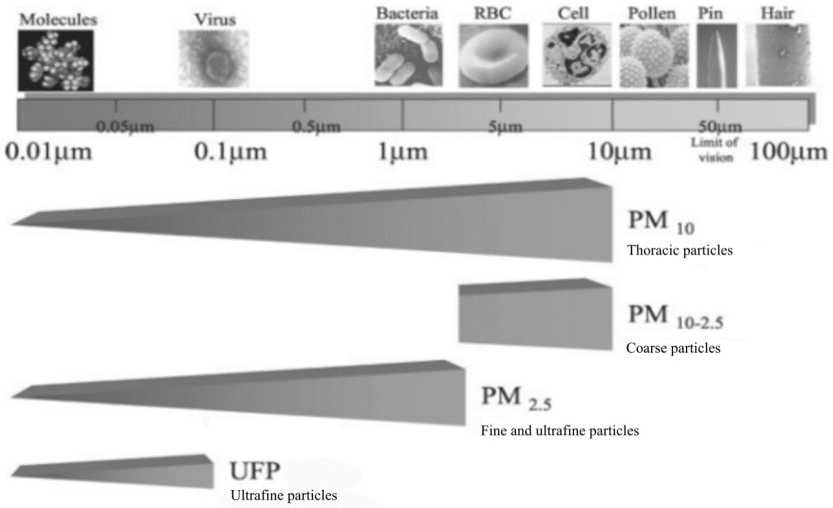

Figure 1 Particulate matter (PM) is categorized according to aerodynamic diameter (size) and how far it can penetrate the lungs. *The coarse particles with a size up to 10 µm will deposit in the throat and are often coughed or sneezed out. Fine particles and ultrafine particles are designated $PM_{2.5}$ and have a size range from 2.5 µm to 0.01 µm and can reach the alveoli and terminal bronchioles. Picture adapted from (Brook et al., 2004).*

PM is a significant contributor to air pollution, and studies suggest it may affect our health primarily through the respiratory tract. Inhaled PM may lead to lung cancer and other respiratory diseases, including reduced lung function, exacerbation of asthma, increased morbidity of obstructive lung diseases, and also cardiovascular diseases (Quay, Reed, Samet, & Devlin, 1998; Ristovski et al., 2012). Studies also suggest a link between $PM_{2.5}$ and various non-communicable diseases (NCDs), including diabetes, hyperactivity disorder, and autism in children (Landrigan et al., 2018). One significant contributor to $PM_{2.5}$ in urban air is the combustion of diesel, which causes the emission of DPM.

1.2.1. Diesel particulate matter (DPM)

The usage of diesel engines in vehicles is one of the critical contributors to DPM in the air and is one of the primary sources of exposure to humans (Wichmann, 2007). DPM consists of $PM_{2.5}$ and is a complex mixture of solid and liquid particles suspended in the gas, meaning that DPM might reach deep into the lungs (Ristovski et al., 2012; Wichmann, 2007). The variations in chemical composition and sizes of the particles among engines make the potential toxicity of DPM not easily understood (Wichmann, 2007). Accordingly, the $PM_{2.5}$ consists of a carbonaceous part other substances can condense on, including sulfates, metallic substances, and inorganic and organic chemicals (Ristovski et al., 2012), which may alter the toxic

potential. One primary organic chemical group is the PAHs, which are linked to many of the toxic effects seen after exposure to $PM_{2.5}$ and DPM (Ristovski et al., 2012; Wichmann, 2007).

1.2.2. Polycyclic aromatic hydrocarbons (PAHs)

PAHs are composed of fused benzenoid rings having different properties, including being semivolatile (Boström et al., 2002). Some of the smaller 2-3 ringed PAHs are predominantly in the gas phase and are associated with coarse particles. Four-ringed PAHs are present in both gas and particulate phases, and the 5-6 ringed PAHs are mainly present in the particulate phase, dominating in $PM_{2.5}$ (Dat & Chang, 2017).

One of the main exposure routes for PAHs is through inhalation, where tobacco smoke seems to be of importance (Lannerö et al., 2008). PAHs are formed during incomplete combustion processes from industry, heating, and carbonaceous particles such as DPM (Boström et al., 2002). Lenner and Karlsson reported that cars having diesel engines might emit five times more PAHs compared to gasoline engines (Lenner & Karlsson, 1998). However, since then, the technology has improved, and diesel engines with filters are suggested to decrease the PAH emission from diesel engines up to 70% (Apicella et al., 2020). Also, in recent times, legislation concerning the amount of PAHs in the air have reduced the presence of these compounds (K.-H. Kim, Jahan, Kabir, & Brown, 2013). Nevertheless, exposure to PAHs still causes harm to humans (Boström et al., 2002). According to recent studies, occupational exposure to PAHs are possibly associated with a higher risk of adverse health effects, including lung cancer (Olsson et al., 2010). However, it should be noted that exposure to other pollutants may also contribute to the observed adverse health effects. Nitrated PAHs (nitro-PAHs) are also known to have carcinogenic properties and are formed through nitration reactions of the combustion-generated PAHs (IARC, 2014; Nowakowski, Rostkowski, & Andrzejewski, 2017).

Nitrated polycyclic aromatic hydrocarbons (nitro-PAHs)

Nitro-PAHs are formed during photochemical and atmospheric processes, produced by a chemical reaction between the PAHs and NO_X (Boström et al., 2002; IARC, 2017). It has previously been suggested that several PAHs and nitro-PAHs might be crucial human cell mutagens in the aerosol extracts (Durant, Busby, Lafleur, Penman, & Crespi, 1996). Furthermore, the metabolic activation of PAHs and nitro-PAHs by the Cytochrome P450 (CYP) enzyme 1A1 (CYP1A1) and 1B1 (CYP1B1) may induce their toxic potential through the

formation of reactive electrophilic metabolites (e.g., epoxides) as well as reactive oxygen species (ROS) (Y.-D. Kim, Ko, Kawamoto, & Kim, 2005; Namazi, 2009).

1.2.3. Reactive oxygen species (ROS)

ROS, or oxygen radicals, may not only be formed during the metabolism of xenobiotics but are also produced during aerobic metabolism and may increase as a result of incomplete reduction of oxygen (O_2) to water (H_2O). Oxygen radicals include superoxide anion radical (O_2^-), hydrogen peroxide (H_2O_2), and hydroxyl radical ($^{\bullet}OH$) (Smart & Hodgson, 2018). The imbalance between the production of ROS and the available antioxidant defenses may cause oxidative stress (Ristovski et al., 2012), having the potential to cause damage to DNA, proteins, lipids, and other molecules (Namazi, 2009; Simon, Haj-Yehia, & Levi-Schaffer, 2000).

Because of the oxygen radicals' small, diffusible size, rapid synthetization, and removal, they can also work as second messengers in important cellular signaling events. However, they are also toxic at high concentrations, making them efficient only at a narrow concentration range (Schreck & Baeuerle, 1991; Schreck, Rieber, & Baeuerle, 1991). Notably, the production of oxygen radicals can be triggered by immune cells, which are important during inflammation as a part of the defense mechanism (Gamaley & Klyubin, 1999; Simon et al., 2000).

1.3. The immune system

The immune system's main task is to recognize self from non-self, accordingly, by identifying proteins and molecules belonging to the body and foreign bodies such as bacteria, viruses, and toxic compounds (Murphy & Weaver, 2017a). Notably, the immune system may also react to PM, where the attached PAHs are reported to have an essential role in inducing inflammatory responses (Bonvallot et al., 2001).

The immune system is separated into the innate (first line of defense) and the adaptive (second line of defense). The innate immune system consists of anatomical barriers, such as the physical and chemical barrier of the respiratory system, and more specialized innate immune cells, modulating the innate immune response. The innate immune cells are different types of white blood cells (leukocytes), which are characterized by moving into the circulatory system to protect the body from harm (Parham, 2015a). Furthermore, the immune cells communicate

with each other, and with non-immune cells, such as epithelial cells, by cytokine production and release, which triggers immune responses. (Whitsett & Alenghat, 2015).

1.3.1. The anatomical barrier of the respiratory system

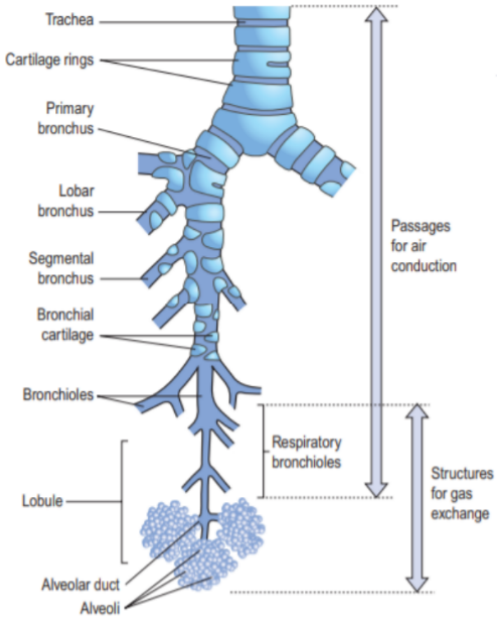

Figure 2 Anatomy of the lower respiratory tract. *The respiratory system is composed of the upper respiratory tract and the lower respiratory tract. The lower includes trachea, bronchus, bronchioles and the gas exchanging part (respiratory bronchioles, alveolar duct and alveoli). Picture taken from (Waugh & Grant, 2014).*

The respiratory system consists of the upper and lower respiratory tract. The lower includes trachea, bronchus, bronchioles, and the gas exchanging part, as shown in Figure 2 (Waugh & Grant, 2014).

The human airway is composed of hollow tubules lined by ciliated, brush, goblet, and basal cells, which structure a physical, secretory, and regulatory barrier of the epithelium, protecting the lungs and airway from inhaled pathogens and environmental pollutants (Cao, Chen, Dong, Xie, & Liu, 2020). Airway epithelial cells respond to these invaders by regulating the inflammatory response through cytokine release (Proud & Leigh, 2011).

Basal cells are stem cells responding to injury by differentiating into goblet cells and ciliated cells, which have important roles in repair responses. Goblet cells secrete mucus and mucins in the submucosal glands (Whitsett & Alenghat, 2015), and ciliated cells dominate in the airway epithelium. Together they constitute the first line of defense (Cao et al., 2020). Furthermore, they are located in the submucosa layer underneath the epithelium layer (Figure 3) (Waugh & Grant, 2014).

Mucins serve a role in maintaining airway homeostasis and removing pollutants by binding and disrupting aggregation and blocking the pollutants' ability to reach underlying epithelial surfaces (Whitsett & Alenghat, 2015). Mucins and mucus provide the mucus gel layer, an essential component of the mucociliary escalator, which traps unwanted particles. The synchronized beating of ciliated epithelium cells moves the particles upwards to the larynx to be swallowed or coughed up (Waugh & Grant, 2014). Notably, the overproduction of mucus in the airways is linked to respiratory diseases, such as asthma and chronic obstructive pulmonary disease (COPD) (Aikawa, Shimura, Sasaki, Ebina, & Takishima, 1992; Whitsett & Alenghat, 2015).

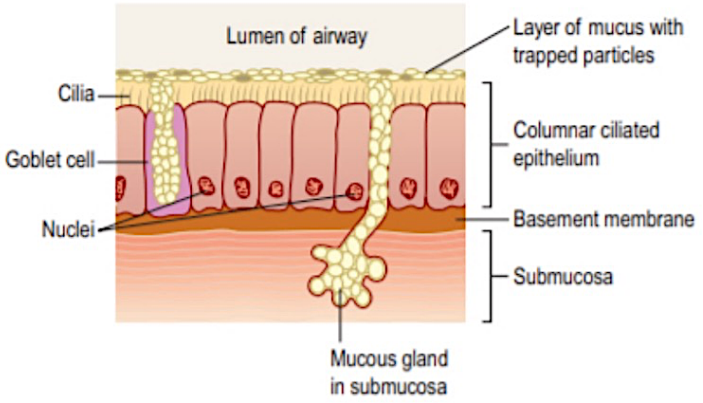

***Figure 3 Structure of airway epithelium and the submucosal gland**. Mucins and mucus are secreted from the submucosal gland. They compose the mucus gel layer, an essential component of the mucociliary escalator. Unwanted particles are trapped in the mucus gel layer, and ciliated epithelium cells move the particles upwards to the larynx to be coughed up or swallowed. Picture taken from (Waugh & Grant, 2014).*

1.3.2. Innate immune cells

A significant part of the innate immune response is to destroy invading agents and pollutants by phagocytosis using phagocytic cells, such as macrophages and neutrophils. Activation of macrophages results in an inflammation response releasing cytokines and chemokines, further recruiting cells from the blood into the infected area (Murphy & Weaver, 2017a). Alveolar macrophages are located in the lung alveoli. They have a critical role in the respiratory tract immune system by protecting the lungs from harmful effects by the removal of foreign PM (Miyata & van Eeden, 2011). Neutrophils usually arrive first at the site of infection in response to cytokines released from macrophages (Downey, Worthen, Henson, & Hyde, 1993). In acute pulmonary inflammation, they have an important function in host defense, including the production of oxygen radicals (Downey et al., 1993).

Mast cells are tissue cells commonly found in mucous membranes. They are essential for wound healing and defense against pathogens via the inflammatory response activated through the release of cytokines and granules. Furthermore, they are crucial in pulmonary inflammation,

including asthma (Cruse & Bradding, 2016). Notably, exposure to $PM_{2.5}$ is suggested to increase the cytokine production, and might further induce allergic effects through the cytokine and histamine release (Jin et al., 2019).

Dendritic cells are located in most tissues, including the inner mucosal lining of the lungs. They identify threats and act as messengers for the rest of the immune system by antigen presentation (Parham, 2015a). Other studies have reported that exposure to PM causes the activation and maturation of dendritic cells, which induce the activation of the adaptive immune cells (Pfeffer et al., 2018). Accordingly, it is suggested that dendritic cells act as a bridge between the innate immune system and the adaptive immune system, modulated by T cells and B cells. These cells give a specific response against threats and rely on antigen receptors that recognize structures of individual pathogens (Murphy & Weaver, 2017a).

1.3.3. Cytokines

Cytokines are small proteins essential for intra- and intercellular communication, having a central role in the regulation of the immune system (Murphy & Weaver, 2017b). Cells often release cytokines when exposed to invading agents, but may also be released after exposure to xenobiotics (Parham, 2015b). The cytokine will bind to a specific receptor located on the surface of another cell. The binding induces a cascade of intracellular signals, causing the cell to change behavior, including the upregulation of genes (Parham, 2015b).

Cytokines include interleukins, chemokines, and others (Zhang & An, 2007). Interleukins are generally expressed by leukocytes, which then act on other leukocytes (Zhang & An, 2007). Mainly, they are made by different immune cells, such as macrophages, causing the development and differentiation of T cells and B cells (Mizel, 1989). Chemokines are chemoattractant cytokines that induce the movement of cells towards the chemokine source. They may be identified by either having two cysteine residues approximate to the amino terminus (CC chemokines) or by having two cysteine residues separated by a single amino acid (CXC chemokines) (Murphy & Weaver, 2017b).

Studies suggest that some pro-inflammatory cytokines, including interleukin 6 (IL-6) and interleukin 8 (CXCL8), are released from airway epithelial cells in response to foreign compounds, such as PM (Mills, Davies, & Devalia, 1999; Park & Park, 2009). Also, their

release is modulated through various signaling pathways (Gomperts, Kramer, & Tatham, 2009b).

Interleukin 6 (IL-6)

IL-6 has many purposes and biological activities and is activated in the early inflammatory response. The activation of IL-6 is increased in association with respiratory diseases and has both pro-inflammatory and anti-inflammatory properties (Quay et al., 1998; Schindler et al., 1990). One systemic effect of IL-6 is the rise in body temperature, a fever, caused by alteration of energy mobilization (Parham, 2015b).

Interleukin 8 (CXCL8)

CXCL8 is a member of the CXC-chemokine family and is expressed in every part of the body (Baggiolini, Walz, & Kunkel, 1989). CXCL8 binds to specific chemokine receptors mainly located on neutrophils, causing the activation and movement of neutrophils from the blood against the concentration gradient of CXCL8 towards the site of production (Parham, 2015b). The production and release of CXCL8 may be triggered by many factors, including bacteria, viruses, and other pro-inflammatory cytokines (Baggiolini et al., 1989; Park & Park, 2009).

1.4. Cell signaling pathways

Cellular signaling pathways describe how extracellular signals translate into intracellular processes. Extracellular first messengers, such as cytokines, bind and activate extracellular receptors. They further induce the formation of second messengers, including calcium ions (Ca^{2+}) (Gomperts, Kramer, & Tatham, 2009a). This may initiate a signaling pathway that results in the activation of genes and the production of corresponding proteins.

Many sensory cells and epithelial cells express pattern recognition receptors (PRRs) (Proud & Leigh, 2011). These receptors recognize inflammatory mediators of many microorganisms, such as pathogen-associated molecular patterns (PAMPs), where PRR activation initiates the innate immune response (Murphy & Weaver, 2017a). Notably, in epithelial cells, PRR activation leads to the release of inducible antimicrobial products that work synergistically to kill bacteria, and the CXCL8 response recruits leukocytes releasing additional antimicrobial molecules (Proud & Leigh, 2011). Notably, respiratory epithelial cells are equipped with

toll-like receptors (TLRs), essential PRRs, which has a critical role in driving mucosal immune responses (Whitsett & Alenghat, 2015).

1.4.1. Toll-like receptors (TLRs)

TLRs consist of 10 intra- and extracellular receptors that can recognize the presence of infections from viruses, fungi, parasites, and other pathogens (Parham, 2015b). The activation of TLRs results in a production of pro-inflammatory cytokines, which may initiate an inflammatory response (Lafferty, Qureshi, & Schnare, 2010). The TLR4 is activated by bacterial components, including lipopolysaccharide (LPS) (Parham, 2015b), whereas TLR3 recognizes double-stranded RNA (dsRNA), which characterizes many viral infections (Alexopoulou, Holt, Medzhitov, & Flavell, 2001). Furthermore, activation of TLR3 mediates host-defense responses to respiratory viral pathogens (Whitsett & Alenghat, 2015). Notably, studies have suggested that activating TLR3 with an agonist, alters the cytokine response after PAH exposure (Øvrevik, Refsnes, Holme, Schwarze, & Låg, 2013)

1.4.2. The aryl hydrocarbon receptor (AhR)

The aryl hydrocarbon receptor (AhR) is an intracellular protein that can bind to different molecules such as PAHs and dioxins, causing an up-regulation of CYP-enzymes. It is involved in the metabolization of many xenobiotics and the formation of ROS. However, other implications of AhR-binding may be of importance for the mutagenic and carcinogenic effects caused by DPM (Bach et al., 2015; Whitlock Jr, 1999).

There are three different signaling pathways of AhR (Figure 4); (1) the classical genomic pathway, (2) the non-classical genomic pathway, and (3) the non-genomic pathway (Holme, Brinchmann, Le Ferrec, Lagadic-Gossmann, & Øvrevik, 2019).

The classical genomic pathway of AhR is activated when an inducer, for instance, 2,3,7,8-tetrachlorodibenzodioxin (TCDD), an AhR ligand, enters the cell and binds to the receptor. The inducer-receptor complex enters the nucleus and attaches to the AhR nuclear translocator (ARNT), making an AhR-ARNT complex. This complex binds to xenobiotic response elements (XREs) in the promotor region of the gene of interest (Brinchmann et al., 2018; Timbrell, 2009). Moreover, it leads to the transcription of CYP-enzyme messenger RNAs (mRNAs), such as *CYP1A1*, and further upregulates CYP1A1 enzymes (Timbrell, 2009).

The non-classical genomic pathway of AhR also leads to the translocation into the nucleus where it may associate with other transcriptional factors, including nuclear factor κB (NF-κB). NF-κB is a crucial transcription factor for innate and adaptive immune responses, having roles in cell death and proliferation (Donaldson et al., 2003; Parham, 2015b). Furthermore, it initiates the transcription of genes, such as genes for cytokines, adhesion molecules, and other proteins necessary for inflammatory responses (Parham, 2015b). Notably, the interaction between AhR and NF-κB impacts each other's activity (Tian, Rabson, & Gallo, 2002).

The non-genomic pathway of AhR does not require the binding to ARNT (Matsumura, 2009). In this pathway, the receptor functions as a signaling molecule, and the responses involve activation of protein kinases and mediation of the intracellular Ca^{2+} concentration ($[Ca^{2+}]_i$) responses. Furthermore, this seems to proceed with secondary activation of genes (Brinchmann et al., 2018).

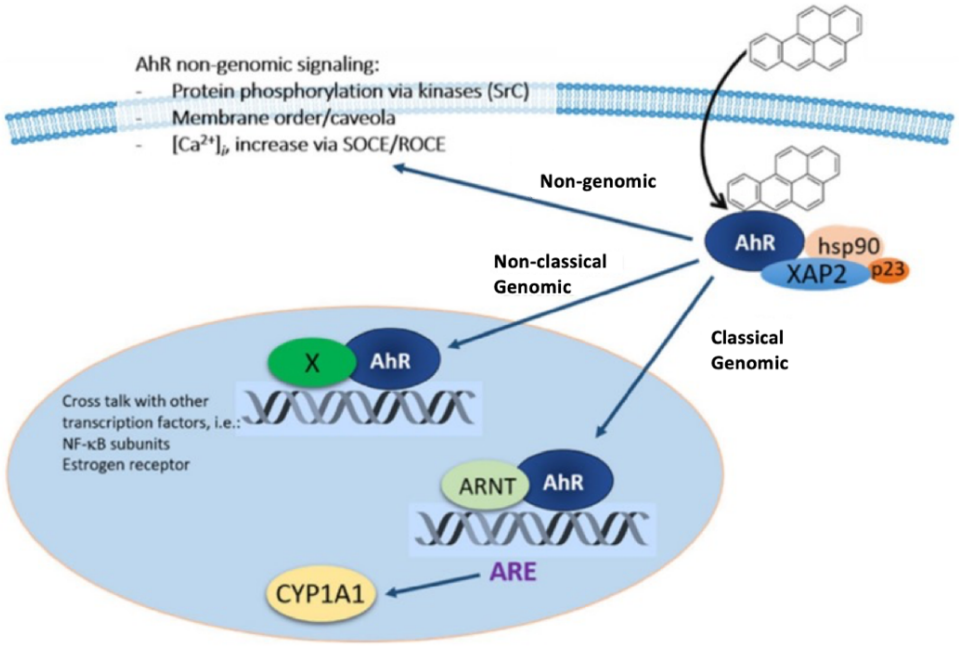

Figure 4 Binding of AhR leads to the upregulation of CYP-enzymes. *Three different signaling pathways are activating AhR. (1) the classical genomic pathway involves the binding of an AhR inducer, such as TCDD, to the receptor. The complex translocates into the nucleus and binds to ARNT, causing the transcription of CYP enzyme mRNA, which further upregulates CYP proteins and enzymes. (2) the non-classical genomic pathway involves the translocation of AhR to the nucleus where it associates with other transcription factors, such as NF-κB, where they modulate each other's activity. (3) the non-genomic pathway is modulated by the receptor working as a signaling molecule and causing activation of protein kinases and the mediation of calcium responses, which further proceeds with the genomic activation of target genes. Figure adapted from (Holme et al., 2019).*

1.4.3. Calcium signaling

Ca^{2+} performs many tasks in cells and is important for the signalization needed to regulate cellular homeostasis. In the lungs, $[Ca^{2+}]_i$ is important for the regulation of cell proliferation, ciliary beat frequency, and mucus and surfactant release (Clapham, 2007). Ca^{2+} also regulates mitochondrial function, motility, and viability. More specifically, an increase in $[Ca^{2+}]_i$ may cause a higher production of adenosine triphosphate (ATP). This reaction may, however, also result in the leakage of free electrons as more oxygen is reduced to water, thereby causing the formation of O_2^- (Clapham, 2007). If too high, this increased production of oxygen radical molecules may induce cell death, which is often found to be a mixture of necrosis and apoptosis (Simon et al., 2000).

1.4.4. Cell death

The different cell deaths are distinguished from each other by morphology. Apoptosis is a form of controlled cell death, mediated by proteolytic enzymes. The morphology includes cell shrinkage, nuclear DNA fragmentation, and membrane blebbing (Tekpli, Holme, Sergent, & Lagadic-Gossmann, 2013). Necrosis, a passive mode of cell death, occurs when there are acute injuries to the cells or extreme physicochemical injuries, such as heat and irradiation (Tekpli et al., 2013). Other types of necrosis also occur in normal cell physiology and development. The symptoms of necrosis consist of damage to the plasma membrane, loss of intracellular homeostasis (Tekpli et al., 2013), and swelling of organelles (Kroemer et al., 2009).

2. Aims of Study

It has been hypothesized that the inflammatory response in cells activated by PM is modulated by the PAHs. Therefore, the overall aim of the project was to explore interactions between various PAHs regarding gene expression with a specific focus on inflammatory responses.

In the present study, we first hypothesized that various PAHs could modify the AhR classical genomic pathway as measured by the expression of *CYP1A1* alone and in combination with the AhR agonist B[*a*]P. Next, we hypothesized that exposure to the PAHs alone or in combination with the TLR3 ligand polyinosinic:polycytidylic acid (Poly I:C) could modify inflammatory responses via AhR. We formulated several working hypotheses:

First, different PAHs might either work as antagonists or agonists towards the classical genomic pathway of AhR.

- The different PAHs alone may modify *CYP1A1* expression
- The PAHs will modify B[*a*]P-induced *CYP1A1* expression

Secondly, various PAHs may modify the release of pro-inflammatory cytokine responses

- PAH exposure may modify IL-6 and CXCL8 release in unprimed cells
- PAH exposure will modify IL-6 and CXCL8 release in Poly I:C primed cells

Thirdly, pyrene may modulate the release of pro-inflammatory cytokine responses via AhR

- CH223191 will reduce the IL-6 and CXCL8 release in unprimed cells
- CH223191 will reduce the IL-6 and CXCL8 release in Poly I:C primed cells

Fourthly, the effects of the PAHs may modify the release of cytokines by changing their gene expression

- Pyrene will increase *IL-6* and *CXCL8* expression in unprimed cells
- Pyrene will increase *IL-6* and *CXCL8* expression in Poly I:C primed cells
- CH223191 will inhibit the expression of *IL-6* and *CXCL8* induced by pyrene in both unprimed and primed cells

Finally, we hypothesized that B[*a*]P and pyrene will activate AhR through the non-genomic pathway.

- B[*a*]P and pyrene will increase the level of intracellular Ca^{2+}

3. Materials and Methods

3.1. Materials

3.1.1. Materials and solutions

The materials and solutions used in the current study are shown in Appendix C and Appendix D.

3.2. Methods

3.2.1. Cell line treatment

In the present study, we used the SV-40 transformed bronchial epithelial cell line, BEAS-2B, derived from healthy human lungs. The BEAS-2B cells (ATCC) were grown at 37°C with 5% CO_2 atmosphere and passaged twice per week. The cells were cultured in serum-free LHC-9 medium on collagen-coated culture flasks. The experiments were executed on near confluent cells in LHC-9 medium for cytokine release and gene expression, and in HHBS (Hank's buffer with Hepes) buffer for Ca^{2+} release measuring.

Priming with the immunostimulant Poly I:C

The synthetic analog of double-stranded viral RNA, Poly I:C, is a TLR3 agonist used to determine if a viral infection can be a confounding factor to the cell's response after exposure to toxic agents and chemicals (Alexopoulou et al., 2001). Poly I:C was purchased from Sigma-Aldrich, and cells were primed with Poly I:C 30 min before exposure to selected compounds.

AhR inhibitor treatment (CH223191)

The well-known AhR antagonist, CH223191, is the first reported ligand-selective antagonist of the AhR having no affinity towards other receptors ("CH223191", n.d.). CH223191 was purchased from Sigma-Aldrich, and the cells were treated with CH223191 for 30 min before exposure to selected compounds.

PAH exposure

BEAS-2B cells were exposed to eight different PAHs known to be abundant in DPM and has different properties and sizes ranging from three to five benzene rings (Figure 5). The PAHs used in this study; phenanthrene, 1-methylphenanthrene (1-MP), fluoranthene, pyrene, 1-nitropyrene (1-NP), β-naphthoflavone (β-NF), benzo[*a*]pyrene (B[*a*]P), and benzo[*e*]pyrene (B[*e*]P). They were purchased at different manufactures (see Appendix C) and dissolved in dimethyl sulfoxide (DMSO), having a DMSO concentration below 1% for all treatments. Also, all the experiments had a negative vehicle control treated with DMSO only.

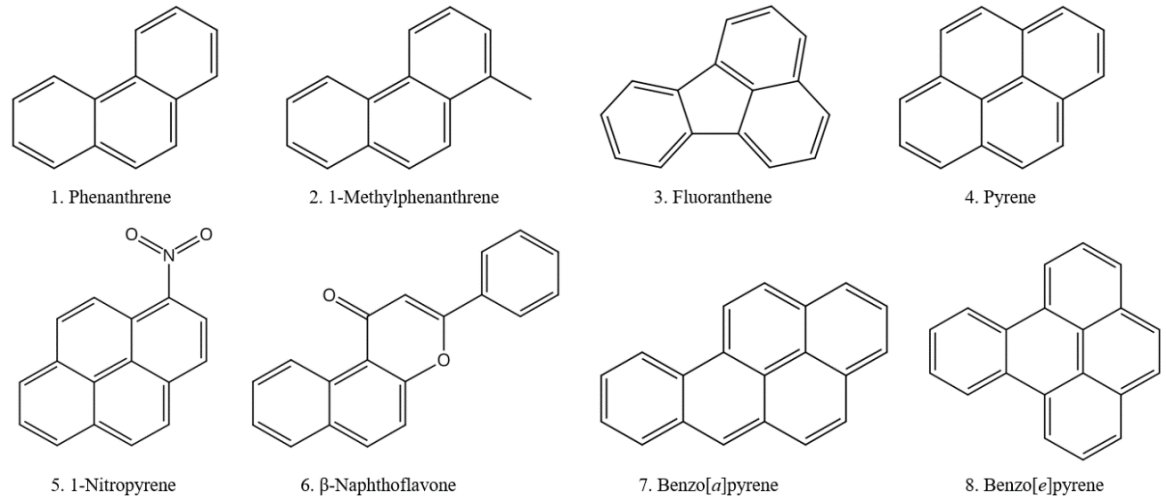

***Figure** 5 **Structures of the PAHs tested.** The PAHs used in this study consisted of three to five fused benzene rings. These were chosen because of their abundancy in diesel exhaust and by having different properties, giving a broader understanding of how different structures modulate different responses. Structures were found at ("SciFinder", n.d.).*

3.2.2. Cytotoxicity (LDH assay)

Cytotoxicity was calculated by measuring lactate dehydrogenase (LDH) activity in the cell culture supernatant. LDH is a cytosolic enzyme present in the cytoplasm of almost all cells of the body. Damage to the plasma membrane results in the release of LDH into the surroundings, making the LDH concentration in cell-free supernatant proportional to the number of dead/damaged cells ("Cytotoxicity Detection Kit (LDH)", n.d.).

LDH is measured using a reaction mixture containing 98% dye solution and a 2% catalyst. The dye solution is composed of 2-(4-iodophenyl)-3-(4-nitrophenyl)-5-phenyl-2H-tetrazolium (INT) and sodium lactate. The catalyst contains diaphorases (dehydrogenase enzymes) and an NAD^+ mixture. The LDH release is quantified by a coupled enzymatic reaction, where LDH

transfers hydrogen when catalyzing the oxidation of L-lactate to pyruvate via reduction of NAD^+ to NADH and H^+ (Tietz, 1985). Diaphorases uses NADH to reduce INT to a red formazan product, where the amount is proportional to the amount of released LDH. Lastly, the maximum leakage of LDH is quantified by making a max LDH control by inducing lysis to the cells by adding 2% Triton-X to non-treated cells, making all the produced LDH to leak out.

The LDH assay (Roche) was conducted by diluting an LDH concentrate solution (10 000 mU/mL) twice in medium, ending up with a primary stock of 1000 mU/mL. The primary stock was series diluted, forming the standard curve concentrations (mU/mL): 1000, 500, 250, 125, 62.5, 31.3, 15.8, and 0. Next, 50 µL of standard dilution and samples were added to a 96-well maxisorb plate. The max LDH control was diluted (1:2, 1:4, and 1:8) and added on the 96-well maxisorb plate together with samples and a negative control containing medium. The color reaction was started by adding 50 µL of the reaction mixture to each well. Afterward, the plate was incubated in a dark place at room temperature for approximately 15 min. Absorbance was measured at 490 nm using TECAN Sunrise Remote Microplate Reader.

3.2.3. Viability (AlamarBlue assay)

Cell viability was measured using the AlamarBlue assay, a method using fluorescence to detect the metabolic activity of cells. It is based on the reduction of the blue poorly fluorescent compound resazurin (oxidized form: 7-hydroxy-3H-phenoxazin-3-1-10-oxide) to the red highly fluorescent colored compound resorufin (reduced form: 7-Hydroxy-3*H*-phenoxazin-3-one) by mitochondrial enzymes carrying diaphorase activity (Zachari et al., 2014).

In short, the AlamarBlue solution (Invitrogen) was diluted 1:10 in HHBS buffer, and 100 µL was added to each well containing cells, including a well without cells (negative control/blank). Afterward, the plate was incubated at 37 °C with 5% CO_2 for 90 min. Fluorescence was measured at Ex/Em = 530/590 nm using ClarioStar plus. Lastly, the viability (%) was calculated, as shown in Equation 1.

$$Viability\ (\%) = \frac{RFU_{sample} - RFU_{blank}}{RFU_{control} - RFU_{blank}} * 100$$

Equation 1 shows how to calculate the viability (%) by using the fluorescence measured by the AlamarBlue assay.

3.2.4. Cytokine release (sandwich ELISA)

ELISA is an immunological assay used to quantify a specific protein in a complex mixture using specific antibodies towards the antigen of interest. In a sandwich ELISA, antigens are quantified between two layers of primary antibodies, each detecting a different epitope (antigenic determinant) of the antigen; the capture and detection antibody.

In this study, streptavidin-HRP (horseradish peroxidase) was used as an enzyme label together with a secondary antibody to detect proteins through a color development. HRP, with H_2O_2 (catalysator), oxidizes the chromogenic substrate tetramethylbenzidine (TMB) from a colorless to a blue substrate. Lastly, by adding a stop solution of sulphuric acid (H_2SO_4), the color changes from blue to yellow (Figure 6).

In short, sandwich ELISA (Invitrogen) was used for detecting the release of IL-6 and CXCL8 after exposing cells in coated 6-well culture dishes for 20 h to selected compounds. First, the wells of a 96-well maxisorb plate were coated with the capture antibody. After 12 h, the plate was washed and incubated 1 h with blocking buffer. A dilution series made the standard curves for IL-6 and CXCL8 (Table 1), and 100 µL of the standard concentrations and diluted samples were added to the maxisorb plate in two parallels before 2 h incubation with 50 µL detection antibody. Afterward, the plate was washed, and HRP was added before 30 min incubation in a dark place. Next, the unbound enzyme was removed by washing before adding the TMB solution. The reaction was stopped with H_2SO_4 after approximately 20 min, and absorbance was measured at reference wavelength 620 nm and absorbance wavelength 450 nm using TECAN Sunrise Remote Microplate Reader.

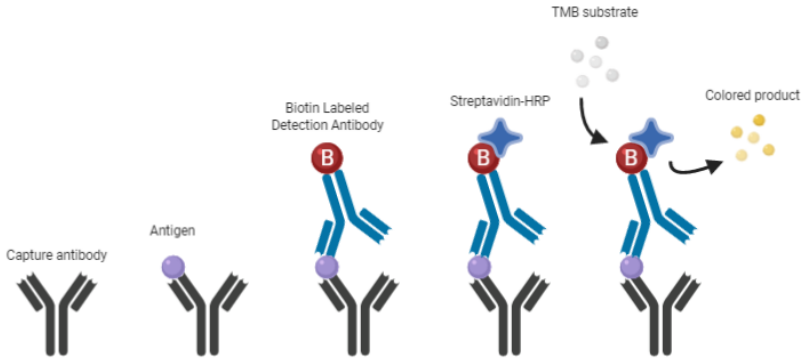

Figure 6 The steps of a sandwich ELISA. *The well is first coated with the capture antibody and afterward incubated with the samples and detection antibody. The cytokine measured will bind to the capture antibody, and the detection antibody with the linked enzyme (HRP) will bind to the antigen. Afterward, the substrate for the linked enzyme is added and causes a measurable color change. The figure is adapted from ("Sandwich ELISA protocol", 2019).*

Table 1 Standard dilution concentrations of IL-6 and CXCL8 used to form the standard curves for the sandwich ELISA assay.

IL-6 (pg/mL)	1000	500	250	125	62.25	31.13	15.56	0
CXCL8 (pg/mL)	800	400	200	100	50	25	12.50	0

3.2.5. Gene expression (Cell-to-C_T)

Cell-to-C_T is a quantitative reverse transcription polymerase chain reaction (RT-qPCR), used to run reverse transcription and qPCR (real-time) directly on the lysate of seeded cells, without any RNA-isolation step. The targeted mRNA is reverse-transcribed to a complementary DNA (cDNA) molecule by reverse transcriptase, an RNA-dependent DNA polymerase enzyme. The newly transcribed cDNA is used as a template for the PCR process and is amplified to the gene of interest. The conventional PCR process consists of cycles of three steps:

1. **Denaturation:** increasing temperature separates the strands
2. **Annealing:** Decreasing temperature attaches primers to their complementary strand of the DNA sequence
3. **DNA synthesis:** Increasing temperature activates the DNA polymerase to synthesize the DNA sequence

The amount of amplified PCR product for each cycle is represented in a graph (Figure 7). The DNA synthesis has a linear phase below the threshold (a level above background fluorescence), before reaching the threshold and going into an exponential phase (Oswald, 2019). The intersection between the threshold and the sample graph is called the cycle threshold value (C_t) and represents the PCR cycle number at which the sample's reaction curve intersects the threshold line (Oswald, 2019). Low C_t values indicate high amounts of the target sequence, and high C_t values indicate lower numbers (Oswald, 2019).

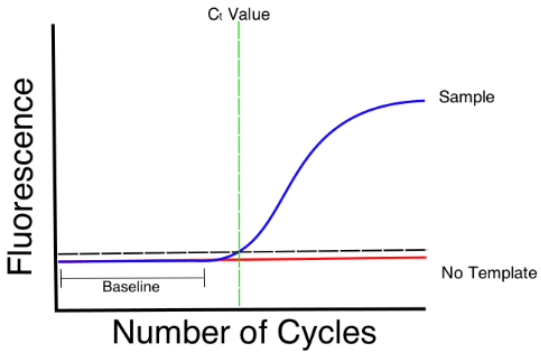

Figure 7 Real-time PCR graph of a sample. *The amplification of PCR products is quantified for each cycle using a fluorogenic mastermix. The quantification can be shown as a graph. The sample graph is linear underneath the threshold value before intersecting with the threshold going into an exponential phase. The threshold value represents the background level of fluorescence, and the intersection with the sample graph (the C_t value) is defined as the number of PCR cycles it takes to detect a real signal from the sample. The picture is taken from (Oswald, 2019).*

Next, the $\Delta\Delta C_t$ method is used to normalize the C_t values by comparing them with a reference gene (18S), such as glyceraldehyde-3-phosphate dehydrogenase (GADPH) (Oswald, 2019). Furthermore, the $\Delta\Delta C_t$ method can be used to calculate fold change, as shown in Equation 2.

$$\Delta C_t = C_{t[gene\ of\ interest]} - C_{t[18S]}$$

$$\Delta\Delta C_t = \Delta C_{t[Treated]} - \Delta C_{t[Control]}$$

$$Fold\ change = 2^{[-\Delta\Delta C_t]}$$

Equation 2 shows the equations used to calculate fold change in gene expression measured by Cell-to-CT.

Cell-to-C_T (Thermofisher Scientific) was used to measure gene expression of *CYP1A1, CXCL8,* and *IL-6.* Cell cultures were seeded two days before and exposed for 5 h to selected compounds in uncoated 96-well culture dishes. After exposure, they were washed with cold phosphate-buffered saline (PBS), aspirated, and stored at −80°C. Next, plates were thawed in room temperature, and 50 µL lysis solution containing 1% DNase were added to the plate, breaking the cells open to access proteins, RNA and DNA, and inactivating endogenous RNases. The plate was incubated for 5 min before adding a stop solution to inactivate the lysis reagents. Lastly, the plate containing the cDNA template was kept on ice, and samples were diluted 1:4. A mastermix (see Appendix D) containing primers (forward and reverse), buffer, DNA polymerase, dNTPs, and water was distributed into a PCR plate before adding the cDNA template. The dNTP mix is fluorogenic, making it possible to detect the specific PCR-product of interest as it accumulates at each PCR cycle. Diluted samples were added to the PCR plate and analyzed with a Bio-Rad CFX96 PCR machine, using the PCR-run shown in Table 2. The expression of the gene of interest was normalized against GADPH and quantified as fold change compared to vehicle control.

Table 2 Steps of the PCR-run

Step	No. of cycles	Temp.	Time (min)
Reverse Transcription	1	48°C	30:00
Polymerase chain reaction	1	95°C	10:00
Amplification	40	95°C	0:15
		60°C	1:00
Plateread between each cycle			
	1	65°C	0:31
Melt curve	61	65°C(+ 0.5°C/cycle, Ramp 0.5°C/s)	0:05
Plateread between each cycle			

3.2.6. Calcium measuring

Cal-520 AM (Abcam) is a fluorogenic calcium-sensitive dye used for detecting intracellular calcium mobilization. It can cross cell membranes, and once inside the cell, the lipophilic blocking groups of Cal-520 AM are cleaved so that it does not escape. The fluorescence is greatly enhanced when binding to intracellular Ca^{2+}, which, upon release, can be detected by measuring the fluorescence ("Cal-520® AM", 2017).

$[Ca^{2+}]_i$ was measured according to the protocol (see Appendix B). In short, 20 000 cells/well were seeded in a black-wall clear-bottom 96-well plate two days before the measurement. On the day of the experiment, the medium was changed, and the cells were incubated for 30 min at 37°C and 5% CO_2 with a dye solution containing 5 μM Cal-520 AM, 0.04% pluronic, and 2.5 mM probenecid in HHBS buffer. After 30 minutes of incubation, the dye solution was removed and replaced with the PAH exposure stocks made in HHBS buffer containing 2.5 mM probenecid. The fluorescence was measured every other minute for 142 min at Ex/Em = 492/514 nm using ClarioStar Plus with 37°C incubation.

3.2.7. Statistical analysis

Mean and standard deviation (SD) are reported for at least three independent experiments and between technical replicates for one-time experiments. Statistical analyzes were conducted for experiments having at least three biological replicates using GraphPad Prism v.8. Data were checked for normality using the Shapiro-Wilk normality test ($p < 0.05$) (Whitlock & Schluter, 2015a). The normally distributed data were analyzed using One-way or Two-way ANOVA. Data that did not follow a normal distribution were analyzed using the non-parametric test Kruskal-Wallis (for one-way ANOVA), or they were log-transformed ($X = \log(X)$) to meet the criteria of normality (Whitlock & Schluter, 2015a). Furthermore, the data were analyzed using repeated measures to exclude interexperimental variations. The multiple comparisons test Bonferroni's, Tukey's, or Dunnett's were used. Bonferroni was used when comparing a set of means (Whitlock & Schluter, 2015b), Tukey, when comparing every mean with every other mean (Tukey, 1949), and Dunnett when comparing the means with the control-mean (Dunnett, 1955). Values of $p < 0.05$ were considered statistically significant.

3.3. Methodological testing

3.3.1. Cell density

Before conducting the cytokine release experiments, we tested the impact of different cell densities (see Appendix A). In short, cells were seeded at 200 000 cells/well and 400 000 cells/well and primed with 3 µg/mL Poly I:C for 30 min before exposure to 3, 10, and 30 µM pyrene one day or two days after seeding. After 20 h exposure, the CXCL8 release was measured by sandwich ELISA. Although just preliminary experiments, not done in sufficient repeat, the results indicate that too high or too low cell density may cause variable results. Notably, it seemed that waiting two days after seeding caused less variability compared to exposure one day after seeding. Therefore, we decided to do the cytokine release experiments seeding out 220 000 cells/well and wait two days before exposing the cells towards the selected compounds.

3.3.2. Calcium measuring

A few pilot studies were also conducted for measuring Ca^{2+} release using Cal-520 AM (see Appendix A). In short, the pilot studies illustrated that extracellular Ca^{2+} is essential for the intracellular Ca^{2+} release. Thus, as recommended, Ca^{2+} was kept available in the HHBS buffer and dye solution during the experiments. Based on these preliminary studies, we decided to use a 30 min loading time with the dye solution and 2.5 mM probenecid in the exposure buffer.

3.4. Methodological considerations

3.4.1. Use of an *in vitro* model

Using *in vitro* cell models is useful for gaining a rapid screening of toxic effects of many chemicals and possible mechanisms involved. In general, *in vitro* methods are cheap and have few ethical difficulties. The methods are reproducible and can be efficiently conducted multiple times to achieve a considerable amount of data in a short time frame. The disadvantage of an *in vitro* method is the low biological and ecological relevance of looking at one or multiple cell lines separately, not showing how the different cells work together.

Most inhaled particles deposits in the bronchial branches, making bronchial epithelial cells a natural target for inhaled air pollution and can be used as a relevant modeling system for air pollution toxicity in humans (Schlesinger & Lippmann, 1978). Earlier studies demonstrate that the immortalized cell line BEAS-2B has a high homology in gene expression when compared to primary cells, and can be used as a surrogate to investigate the metabolism of toxicants in bronchial epithelium (Courcot et al., 2012). In the current study, BEAS-2B was chosen by being robust and easily cultured and maintained when compared to primary cell lines ("Primary Cell Culture Basics", n.d.). However, because immortalized cell lines may have altered standard physiological properties ("Primary Cell Culture Basics", n.d.), it should be considered to supplement the current study using a primary cell line.

3.4.2. Experimental methods

In the current study, the LDH assay was used to measure cytotoxicity. This is a time-efficient assay where it is easy to handle more samples simultaneously, and it is reliable for more extensive experiments. As the LDH assay only measures the amount of leaked LDH, the results can be affected by skewed cell numbers due to reduced cell proliferation. The AlamarBlue assay was used after Ca^{2+} measuring to assess the viability, and by measuring the amount of metabolic activity in the cell population, the results can be affected by the individual cell reducing ability and by agents affecting mitochondrial activity. Thus, it would be ideal to use these two methods in combination, measuring both cell death and metabolic activity.

Cytokine release *in vitro* can be measured using different methods, including Western blotting and various types of ELISAs. In the current study, we decided to use the reliable and highly quantitative method sandwich ELISA (Leng et al., 2008). This method is less time-consuming compared to Western blotting and more reliable than the other ELISAs by quantifying the antigen between two layers of antibodies, giving less background noise.

Gene expression *in vitro* is usually quantified by various PCR methods or Northern blotting. Northern blotting is time-consuming, and we, therefore, decided to use a qRT-PCR method, which measures gene amplification in real-time and quantifies the amount of non-specific and primer-dimers formed during the PCR reaction. Also, this method has high sensitivity, specificity, and is time-efficient, making it possible to analyze many samples at once. However, it is an expensive method prone to DNA contamination, and it is only possible to analyze the expression of one gene at the time. In the current study, only technical replicates of exposure were conducted. Ideally, technical replicates of the PCR-run would be included, thus excluding inaccurate measurements, and also to confirm that the PCR-run is successful.

In general, measuring of Ca^{2+} release *in vitro* is accomplished by using fluorescence dyes and further examination through calcium single-cell microscopic imaging. However, in the current study, a fluorescence dye, Cal-520 AM, was used, and Ca^{2+} release was analyzed by directly measuring fluorescence. The Cal-520 AM dye is relatively new, and the knowledge of using this dye and by only measuring fluorescence is limited. However, it appeared to have worked well in earlier studies (Lock, Parker, & Smith, 2015), which is why this method was chosen. In general, it was a secure method for loading the cells with dye, and measurement was efficiently conducted using a fluorescence microplate reader. Nevertheless, the calcium single-cell microscopic imaging is a more sensitive method, which probably would have been a better choice according to earlier knowledge. Also, positive control should have been included to calculate the actual amount of Ca^{2+} release and not only the changes in fluorescence.

4. Results

4.1. The PAHs modulates *CYP1A1* expression

We tested if the various PAHs could activate the classical genomic pathway of AhR by inducing *CYP1A1* expression alone or modulate B[*a*]P-induced *CYP1A1* expression. Notably, because β-NF is a well-known AhR agonist, it was excluded from these experiments.

We first checked for cytotoxicity by measuring the cell leakage of LDH (mU/mL) determined by the LDH assay. The cells were treated with the selected PAHs (0.1, 1, and 10 μM) alone and in combination with 0.1 μM B[*a*]P for 5 h and 24 h before the LDH measurement. Neither of the PAHs alone or given in combination with B[*a*]P seemed to cause any marked changes in morphology, as judged by microscopic examination (data not presented). Furthermore, as seen from the results shown in

Figure 8, none of the various exposures seemed to cause any marked changes in cell leakage of LDH after 5 h or 24 h exposure when compared to control (DMSO).

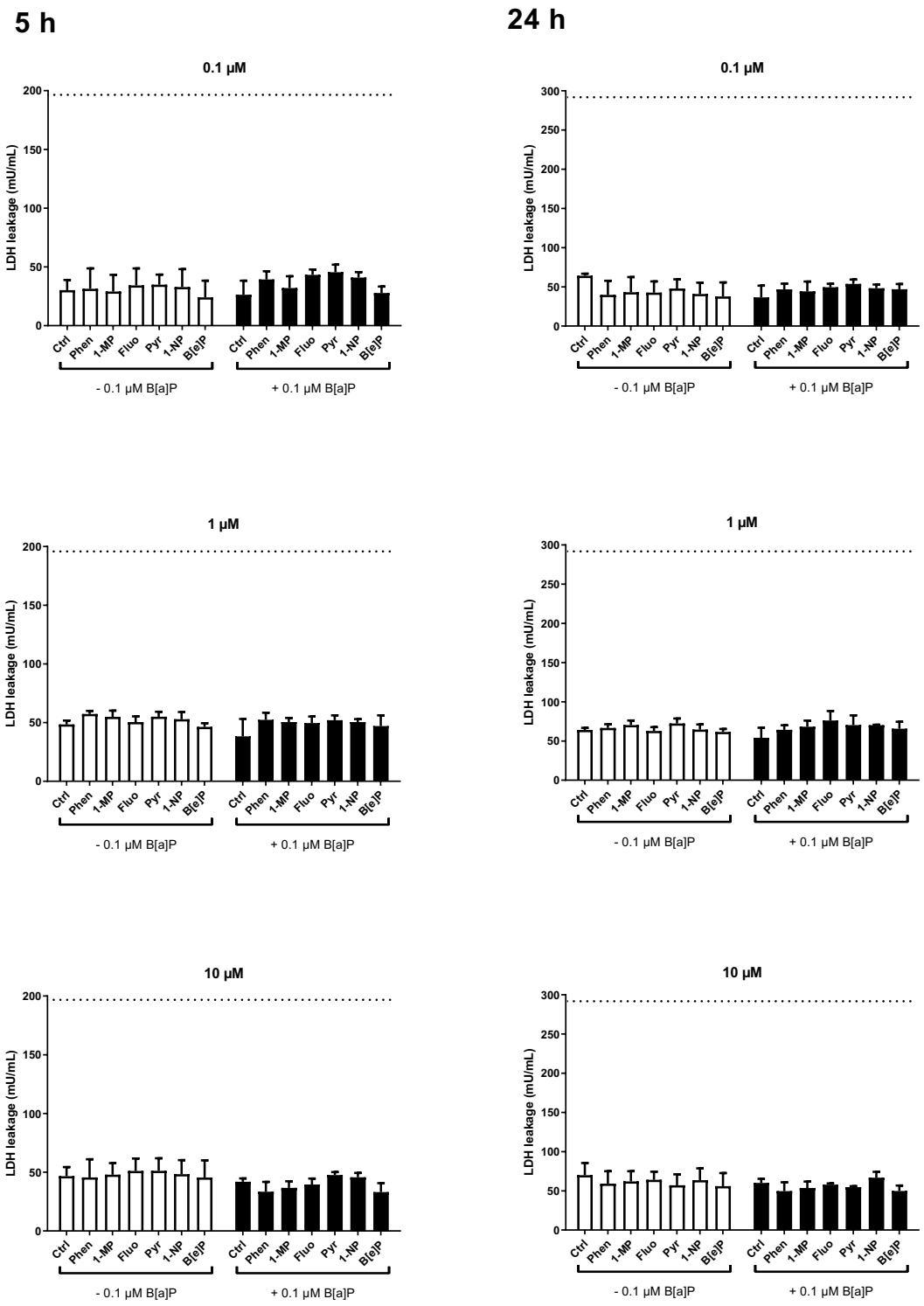

Figure 8 Cell leakage of LDH (mU/mL) after exposing BEAS-2B cells to selected PAHs. *The cells were exposed to 0.1, 1, and 10 µM of the selected PAHs, alone and in combination with 0.1 µM B[a]P. The LDH leakage was determined by the LDH assay. The data are represented as the mean value ± SD of one biological experiment with three technical replicates. The results are shown as the concentration of LDH (mU/mL), where the dotted line represents the max LDH leakage = 196.56 and 291.73 mU/mL for the 5 h and 24 h exposure, respectively. Abbreviations; ctrl = control (DMSO), phen = phenanthrene, 1-MP = 1-methylphenanthrene, fluo = fluoranthene, pyr = pyrene, 1-NP = 1-nitropyrene, B[a]P = benzo[a]pyrene, B[e]P = benzo[e]pyrene.*

First, we examined the effect of B[*a*]P and pyrene alone and in combination, to assess which concentrations would be preferable to use for the other PAHs. The cells were exposed for 5 h to B[*a*]P (0.03, 0.1, 0.3, and 1 µM), and pyrene (0.1, 1, 3, and 10 µM). The *CYP1A1* expression was measured using Cell-to-C_T. As this experiment was a pilot study, we conducted one experiment with three technical replicates. Thus, these results represent the intraexperimental variation. As seen in the results presented in Figure 9, there was a trend of concentration-dependent increase in the *CYP1A1* expression starting already at 0.1 µM B[*a*]P. In contrast, a reduction of *CYP1A1* synthesis appeared after exposure to 1 µM and higher concentrations of pyrene. We further decided to test pyrene (0.1, 1, 3, and 10 µM) in combination with 0.1 µM B[*a*]P. Accordingly, pyrene seemed to reduce the B[*a*]P-induced *CYP1A1* expression in a concentration-dependent manner, starting already at 0.1 µM.

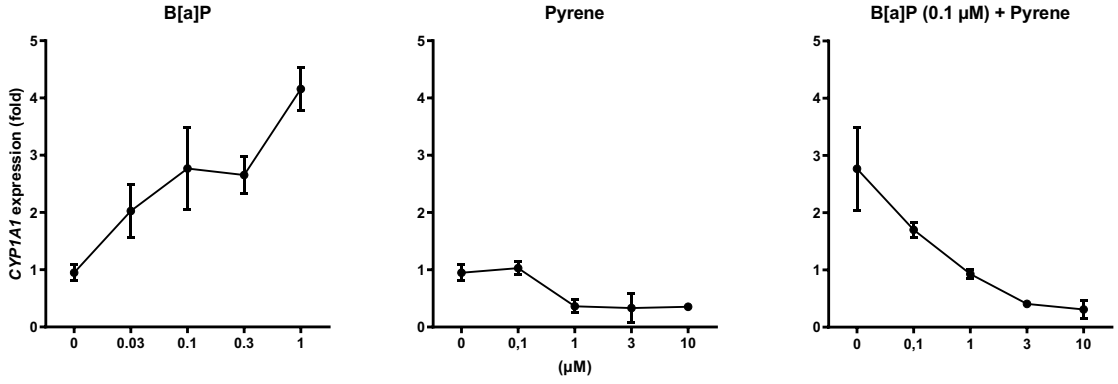

Figure 9 CYP1A1 expression after exposing BEAS-2B cells to B[a]P and pyrene. *The cells were exposed for 5 h to B[a]P (0.03, 0.1 , 0.3 and 1 µM) and pyrene (0.1, 1, 3 and 10 µM) alone, and 0.1 µM B[a]P in combination with pyrene (0.1, 1, 3 and 10 µM). The CYP1A1 expression was determined by Cell-to-C_T. The data are represented as the mean value ± SD of one biological experiment with three technical replicates of exposure, and the results are shown as fold change compared to the control (DMSO).*

As B[*a*]P seemed to increase the *CYP1A1* expression already at a concentration of 0.1 µM, we decided to use 0.1 µM B[*a*]P in combination with the selected PAHs. Furthermore, we decided to use the concentrations 0.1, 1, and 10 µM for the other PAHs, thus covering a relatively wide concentration range. We measured the *CYP1A1* synthesis after 5 h exposure, as presented in Figure 10. Three biological replicates were conducted for the concentrations 0.1 µM and 1 µM, but for the highest concentration (10 µM), only two biological replicates were performed. Therefore, only statistics for 0.1 µM and 1 µM are reported.

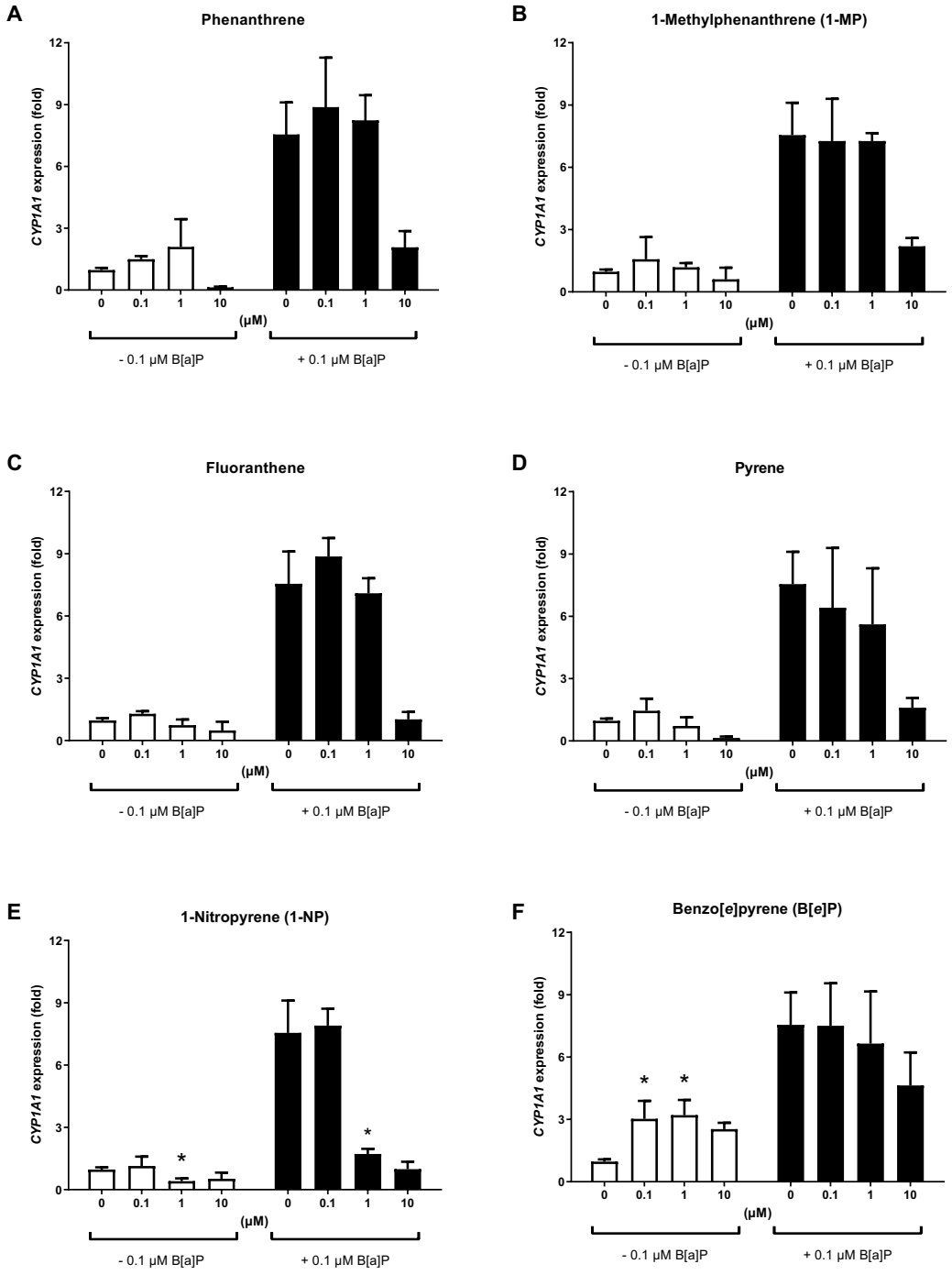

Figure 10 CYP1A1 expression after exposing BEAS-2B cells to the PAHs. *The cells were exposed for 5 h to the selected PAHs (0.1, 1, and 10 µM) alone and in combination with 0.1 µM B[a]P. The CYP1A1 expression was determined by Cell-to-CT. The data are represented as the mean value ± SD of three biologically independent replicates for 0.1 µM and 1 µM, and two for 10 µM, all with three technical replicates of exposure. The results are shown as fold increase of the control. * is a significant difference relative to control, $p < 0.05$ for Two-way ANOVA with Dunnett's multiple comparison test. The statistics were calculated with repeated measures using the ΔΔCt values.*

Phenanthrene appeared to cause a non-significant concentration-dependent increase in *CYP1A1* expression at 0.1 µM and 1 µM, while 10 µM instead caused a trend of reduction (Figure 10A). No changes appeared in the B[*a*]P-induced *CYP1A1* synthesis following 0.1 µM and 1 µM phenanthrene. Whereas, phenanthrene at the highest concentration (10 µM) seemed to cause a reduction in the B[*a*]P-induced *CYP1A1* expression.

Neither of the concentrations of 1-MP (0.1, 1, and 10 µM) alone indicated any trend of change in the expression of *CYP1A1* (Figure 10B). When the cells were exposed to B[*a*]P, 0.1 µM and 1 µM 1-MP did not make any change in B[*a*]P-induced synthesis. In contrast, the highest concentration of 1-MP (10 µM) appeared to decrease the *CYP1A1* expression induced by B[*a*]P. Notably, none of the treatments had a statistically significant effect on the *CYP1A1* synthesis when compared to the control.

As shown in Figure 10C, no marked changes in *CYP1A1* synthesis were observed after exposure to 0.1 µM and 1 µM fluoranthene. In contrast, 10 µM seemed to cause a trend of reduction in *CYP1A1* expression. No changes in the B[*a*]P-induced *CYP1A1* synthesis was observed after exposure to 0.1 µM and 1 µM fluoranthene, whereas the highest concentration (10 µM) seemed to cause a reduction. Notably, none of the treatments had a statistically significant effect on the synthesis of *CYP1A1* when compared to control.

As seen in the results presented in Figure 10D, pyrene appeared to cause a non-significant concentration-dependent decrease in *CYP1A1* expression. When the cells were exposed to B[*a*]P, pyrene seemed to induce a concentration-dependent reduction in the B[*a*]P-induced *CYP1A1* synthesis, although not statistically significant.

Exposure to 0.1 µM 1-NP, as shown in Figure 10E, did not markedly change the *CYP1A1* synthesis. In contrast, 1 µM 1-NP induced a 2-fold and statistically significant reduction in *CYP1A1* expression when compared to control (Dunnett, $p = 0.0008$). Furthermore, 10 µM 1-NP indicated a reduction in the expression of *CYP1A1*. After the exposure to B[*a*]P, 0.1 µM 1-NP did not indicate any change, whereas 1 µM 1-NP significantly decreased the B[*a*]P-induced *CYP1A1* synthesis with a 4-fold (Dunnett, $p < 0.0001$). Also, 10 µM 1-NP appeared to reduce the B[*a*]P-induced *CYP1A1* expression slightly.

As shown in Figure 10F, after exposure to 0.1 µM and 1 µM B[*e*]P, there was a 3-fold and a statistically significant increase in *CYP1A1* expression (Dunnett, p = 0.0009 and 0.0006, respectively). Furthermore, 10 µM B[*e*]P appeared to increase the synthesis slightly. When the cells were exposed to B[*a*]P, no marked changes in the B[*a*]P-induced *CYP1A1* synthesis following any of the concentrations of B[*e*]P were observed.

4.2. The induced cytokine release by the PAHs

Cytokine release after exposure to the PAHs was measured in unprimed and in Poly I:C primed cells. In the current study, we decided to use 3 µg/mL Poly I:C since higher concentrations were found to have slightly cytotoxic effects as judged by microscopic examination (data not presented).

We first wanted to evaluate what concentration of the PAHs would be preferable to use by making a concentration curve of pyrene in both unprimed and Poly I:C primed cells. Thus, we primed the cells with Poly I:C (3 µg/mL) for 30 min before 20 h exposure to pyrene (3, 10, and 30 µM). The results presented in Figure 11 shows the cell leakage of LDH (mU/mL) after the treatments, as measured by the LDH assay. The primed cells had a statistically significant increase in LDH leakage compared to unprimed cells (Bonferroni, p < 0.004). Nevertheless, neither of the concentrations of pyrene in unprimed or primed cells caused any statistically significant change in LDH leakage when compared to their respective controls. The LDH leakage corresponded to approximately 3-5% cytotoxicity in unprimed cells and 7-9% in primed cells.

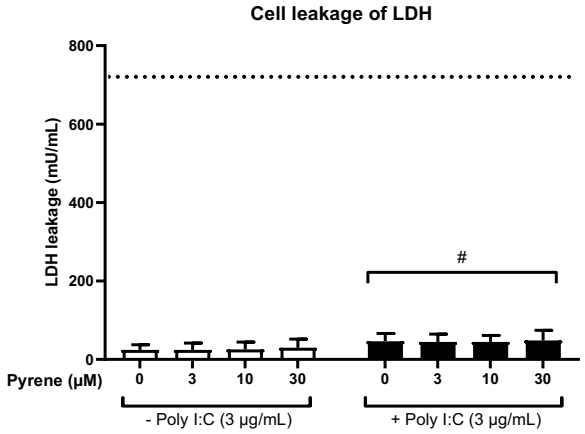

Figure 11 Cell leakage of LDH (mU/mL) after exposing unprimed and primed BEAS-2B cells to pyrene. *The cells were primed with Poly I:C (3 µg/mL) for 30 min and exposed to pyrene (3, 10, and 30 µM) for 20 h. The LDH leakage was determined by the LDH assay. The data are represented as the mean value ± SD of four biological independent replicates with two technical replicates. The results are shown as the concentration of LDH (mU/mL), where the dotted line represents the average max LDH leakage = 728.44 mU/mL. No significant difference relative to control, p < 0.05 for Two-way ANOVA with Dunnett's multiple comparison test. # is a significant difference relative to the unprimed group, p < 0.05 for Two-way ANOVA with Bonferroni's multiple comparison test. The statistics were calculated with repeated measures on log-transformed data.*

Next, we measured IL-6 and CXCL8 release (pg/mL) by sandwich ELISA for the concentration curve of pyrene (Figure 12). Primed cells had a statistically significant increase in release compared to unprimed cells, both for IL-6 and CXCL8 (Bonferroni, $p < 0.0001$, $p = 0.0004$, respectively).

For the unprimed cells, pyrene significantly increased IL-6 release for 10 µM and 30 µM compared to control (Dunnett, $p = 0.008$ and $p < 0.0001$, respectively). For the CXCL8 release, 3 µM pyrene caused a significant reduction (Dunnett, $p = 0.0159$), whereas the higher concentrations of pyrene (10 µM and 30 µM) did not cause any observable change in the CXCL8 response. Pyrene exposure in primed cells appeared to increase IL-6 and CXCL8 release in a concentration-dependent manner. However, only the highest concentration of pyrene (30 µM) caused a statistically significant increase in IL-6 and CXCL8 release when compared to Poly I:C control (Dunnett, $p = 0.0013$, and $p = 0.0159$, respectively).

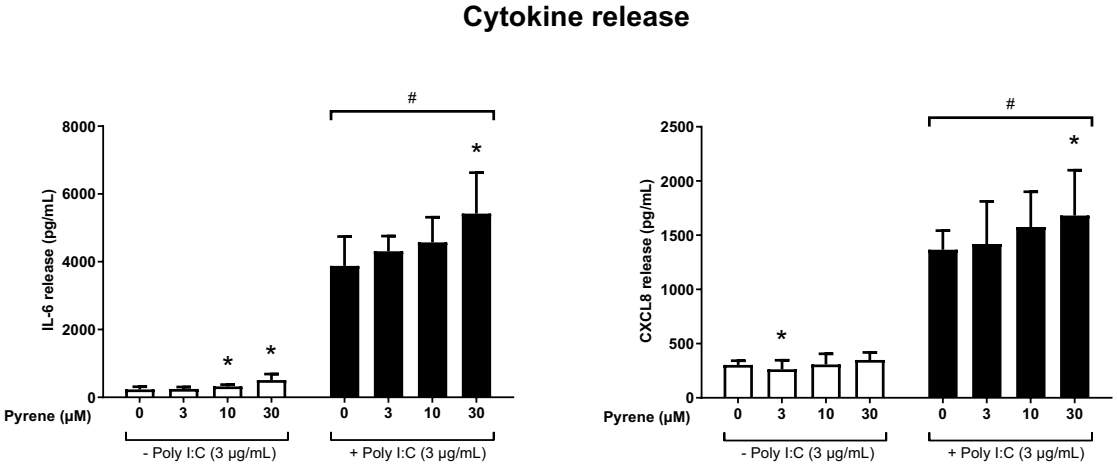

Figure 12 IL-6 and CXCL8 release (pg/mL) after exposing unprimed and primed BEAS-2B cells to pyrene. *The cells were primed with Poly I:C (3 µg/mL) for 30 min and exposed to pyrene (3, 10, and 30 µM) for 20 h. The cytokine release was determined by sandwich ELISA. The data are represented as the mean value ± SD of five biological independent replicates with two technical replicates. The results are shown as IL-6 and CXCL8 release (pg/mL). * is a significant difference relative to control, $p < 0.05$ for Two-way ANOVA with Dunnett's multiple comparison test. # is a significant difference relative to the unprimed group, $p < 0.05$ for Two-way ANOVA with Bonferroni's multiple comparison test. The statistics are calculated with repeated measures and on log-transformed data.*

According to the results presented in Figure 12, we decided to examine the different PAHs further using 10 µM. The cells were unprimed and primed with Poly I:C (3 µg/mL) for 30 min before a 20 h exposure to the PAHs. However, we first checked for cytotoxicity using the LDH assay. The results, shown in Figure 13, represent the measured cell leakage of LDH after 20 h PAH exposure. Primed cells had a statistically significant increase compared to unprimed cells (Bonferroni, p = 0.0155). As for the unprimed cells, neither of the PAHs caused a statistically significant difference in LDH leakage when compared to control, and the leakage corresponded to 3-5% cytotoxicity. In the primed cells, fluoranthene induced a 1.3-fold and statistically significant increase in LDH leakage compared to control (Dunnett, p = 0.0481). The other PAHs (phenanthrene, 1-MP, pyrene, 1-NP, β-NF, B[*a*]P, and B[*e*]P) appeared not to change the LDH leakage. Notably, the LDH leakage after exposure to the PAHs in primed cells corresponded to approximately 7-9% cytotoxicity.

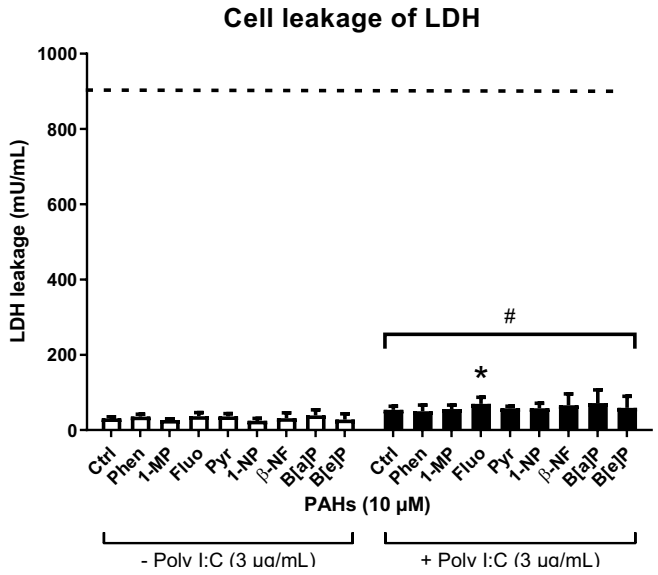

Figure 13 Cell leakage of LDH (mU/mL) after exposing unprimed and primed BEAS-2B cells to various PAHs. *The cells were primed with Poly I:C (3 µg/mL) for 30 min and exposed to the PAHs (10 µM) for 20 h. The LDH leakage was determined by the LDH assay. The data are represented as the mean value ± SD of four biological independent replicates with two technical replicates. The results are shown as the concentration of LDH (mU/mL), where the dotted line represents the average max LDH leakage = 927.39 mU/mL. * is a significant difference relative to control, p < 0.05 for Two-way ANOVA with Dunnett's multiple comparison test. # is a significant difference relative to the unprimed group, p < 0.05 for Two-way ANOVA with Bonferroni's multiple comparison test. The statistics were calculated with repeated measures on log-transformed data. Abbreviations; ctrl = control (DMSO), phen = phenanthrene, 1-MP = 1-methylphenanthrene, fluo = fluoranthene, pyr = pyrene, 1-NP = 1-nitropyrene, B[a]P = benzo[a]pyrene, B[e]P = benzo[e]pyrene.*

The IL-6 and CXCL8 release (pg/mL) after exposure to the PAHs are shown in Figure 14. Accordingly, primed cells significantly increased the IL-6 and CXCL8 release when compared to the unprimed cells (Bonferroni, $p < 0.0001$, and $p < 0.0001$, respectively).

In the unprimed cells, B[*a*]P and β-NF induced a less than 2-fold, but statistically significant increase in IL-6 release (Dunnett, $p = 0.0424$ and $p = 0.0097$, respectively). In contrast, 1-NP appeared to cause a non-significant reduction. A slight non-significant increase in IL-6 also appeared after exposure to B[*e*]P. As for the CXCL8 release, 1-NP caused a 1.5-fold decrease, and β-NF induced a 1.2-fold increase, both statistically significant compared to control (Dunnett, $p < 0.0001$ and $p = 0.0442$, respectively). In contrast, none of the other PAHs seemed to change the CXCL8 release, nor were they statistically significant when compared to control.

For the primed cells, pyrene appeared to induce an increase in IL-6 release, whereas the other PAHs caused no marked changes. Importantly, it should be noted that none of the treatments had a statistically significant effect on the release when compared to control. For the CXCL8 release, both pyrene and fluoranthene induced a less than 2-fold, but statistically significant increase compared to control (Dunnett, $p < 0.0001$ and $p = 0.0218$, respectively). In contrast, the other PAHs appeared not to affect the CXCL8 release, nor were they statistically significant.

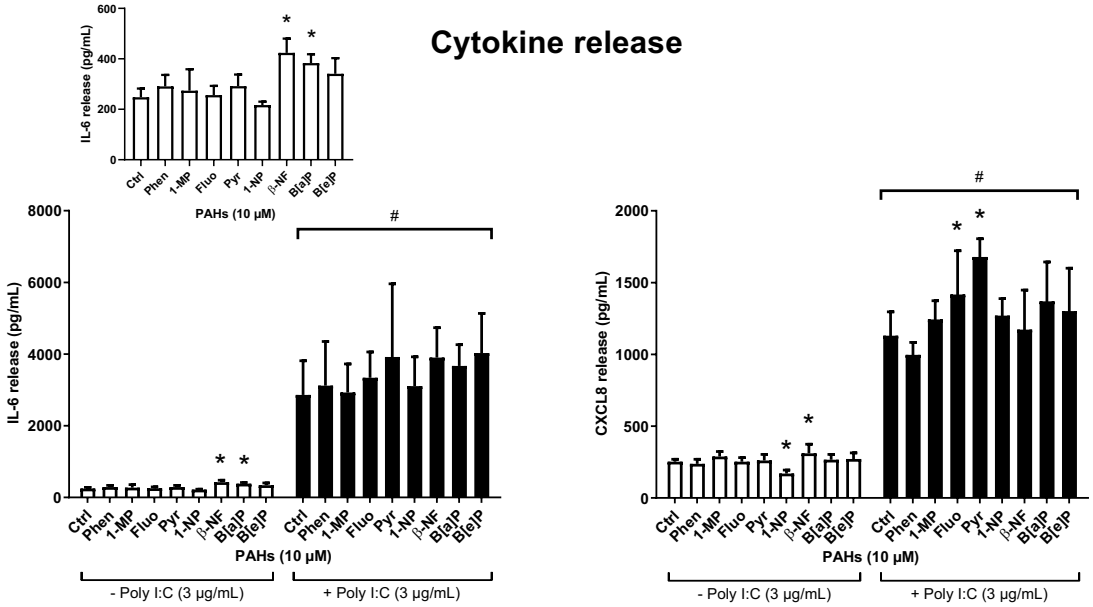

Figure 14 Il-6 and CXCL8 release (pg/mL) after exposing unprimed and primed BEAS-2B cells to various PAHs. *The cells were primed with Poly I:C (3 µg/mL) for 30 min and exposed for 20 h to the PAHs (10 µM). The cytokine release was determined by sandwich ELISA. The data are represented as the mean value ± SD of four biological independent replicates with two technical replicates. The results are shown as an increase in IL-6 and CXCL8 release (pg/mL). * is a significant difference relative to control, $p < 0.05$ for Two-way ANOVA with Dunnett's multiple comparison test. # is a significant difference relative to the unprimed group, $p < 0.05$ for Two-way ANOVA with Bonferroni's multiple comparison test. The statistics were calculated with repeated measures on log-transformed data. Abbreviations; ctrl = control (DMSO), phen = phenanthrene, 1-MP = 1-methylphenanthrene, fluo = fluoranthene, pyr = pyrene, 1-NP = 1-nitropyrene, B[a]P = benzo[a]pyrene, B[e]P = benzo[e]pyrene.*

4.3. The signaling pathway of cytokine release

Next, we examined if AhR activity could modulate the IL-6 and CXCL8 release in unprimed and Poly I:C primed cells by treating the cells with the AhR antagonist CH223191. The cells were primed with Poly I:C (3 µg/mL) and treated with CH223191 (10 µM) for 30 min before 20 h exposure to pyrene (10 µM). Four different treatment groups were conducted; (1) unprimed cells were exposed to pyrene, (2) unprimed cells were treated with CH223191 and exposed to pyrene, (3) primed cells were exposed to pyrene, and (4) cells were primed and treated with CH223191 before exposure to pyrene.

We first measured cell leakage of LDH (mU/mL) using the LDH assay (Figure 15). Pyrene appeared to have approximately the same level of LDH leakage compared to control, and it corresponded to roughly 3-5% cytotoxicity. Treating the cells with CH223191 before exposure to DMSO and pyrene seemed to increase the LDH leakage slightly. However, only pyrene caused a significant increase when compared to control (Dunnett, p = 0.0005). Primed cells exposed to both DMSO and pyrene caused a statistically significant increase in LDH leakage when compared to control (Dunnett, p = 0.0013, and p = 0.0011, respectively), which corresponded to approximately 7-9% cytotoxicity. Lastly, treating the primed cells with CH223191 caused a statistically significant increase in LDH leakage for both DMSO and pyrene exposure when compared to control (Dunnett, p < 0.0001), and corresponded to roughly 15-20% cytotoxicity.

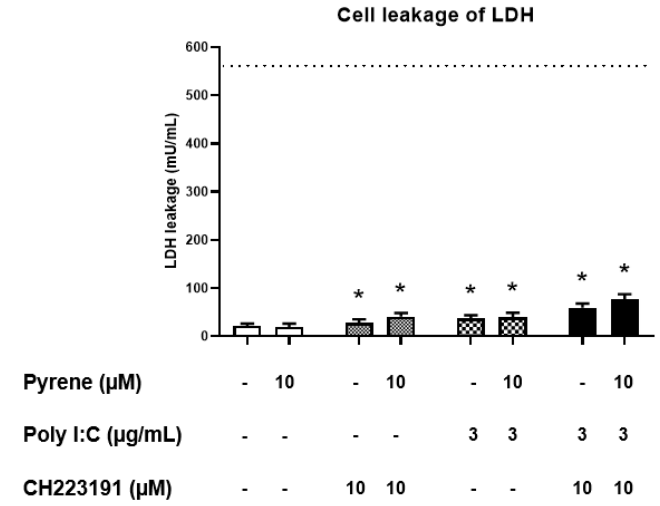

Figure 15 Cell leakage of LDH (mU/mL) after exposing unprimed and primed BEAS-2B cells to pyrene and using the AhR antagonist CH223191. *The cells were primed with Poly I:C (3 µg/mL) alone and in combination with CH223191 (10 µM) for 30 min and exposed to pyrene (10 µM) for 20 h. The LDH concentration was determined by the LDH assay. The data are represented as the mean value ± SD of four biological independent replicates with two technical replicates. The results are shown as the concentration of LDH (mU/mL), where the dotted line represents the average max LDH leakage = 559.08 mU/mL. * is a significant difference relative to control (DMSO), p < 0.05 for Two-way ANOVA with Dunnett's multiple comparison test. The statistics were calculated with repeated measures.*

Figure 16 presents the results of the IL-6 and CXCL8 release (pg/mL) for the four treatment groups. For the IL-6 release, CH223191 caused a 4.7-fold significant reduction, whereas priming the cells caused a 13.9-fold significant increase when compared to control (Tukey, p < 0.0001, p < 0.0001, respectively). Pyrene induced a 1.5-fold increase in IL-6 release when compared to the control (Tukey, p = 0.0153). Also, CH223191 caused a 5.2-fold significant reduction in the pyrene-induced IL-6 release (Tukey, p < 0.0001). In contrast, priming the cells significantly increased the pyrene-induced IL-6 release with a 10.7-fold (Tukey, p < 0.0001), and CH223191 significantly reduced IL-6 release with a 12.8-fold in primed cells (Tukey, p < 0.0001). CH223191 also had a reducing effect on the primed cells exposed to pyrene, and

significantly decreased the IL-6 release with 8.3-fold (Tukey, $p < 0.0001$). There was also a significant increase in primed cells treated with CH223191 and exposed to pyrene compared to primed cells only treated with CH223191 (Tukey, $p = 0.0016$).

For the CXCL8 release, CH223191 caused a 1.8-fold significant reduction when compared to control (Tukey, $p = 0.0036$). Furthermore, CH223191 significantly reduced the pyrene-induced release with a 1.8-fold (Tukey, $p = 0.0127$). In contrast, primed cells induced a 4.4-fold significant increase in CXCL8 release compared to control (Tukey, $p = 0.0032$). Also, priming the cells significantly increased the pyrene-induced CXCL8 release by a 4.8-fold (Tukey, $p = 0.0021$), and CH223191 significantly reduced the release by a 3.8-fold compared to primed cells (Tukey, $p = 0.0124$). For the primed cells exposed to pyrene, CH223191 significantly reduced the CXCL8 release with a 3.7-fold (Tukey, $p = 0.0021$).

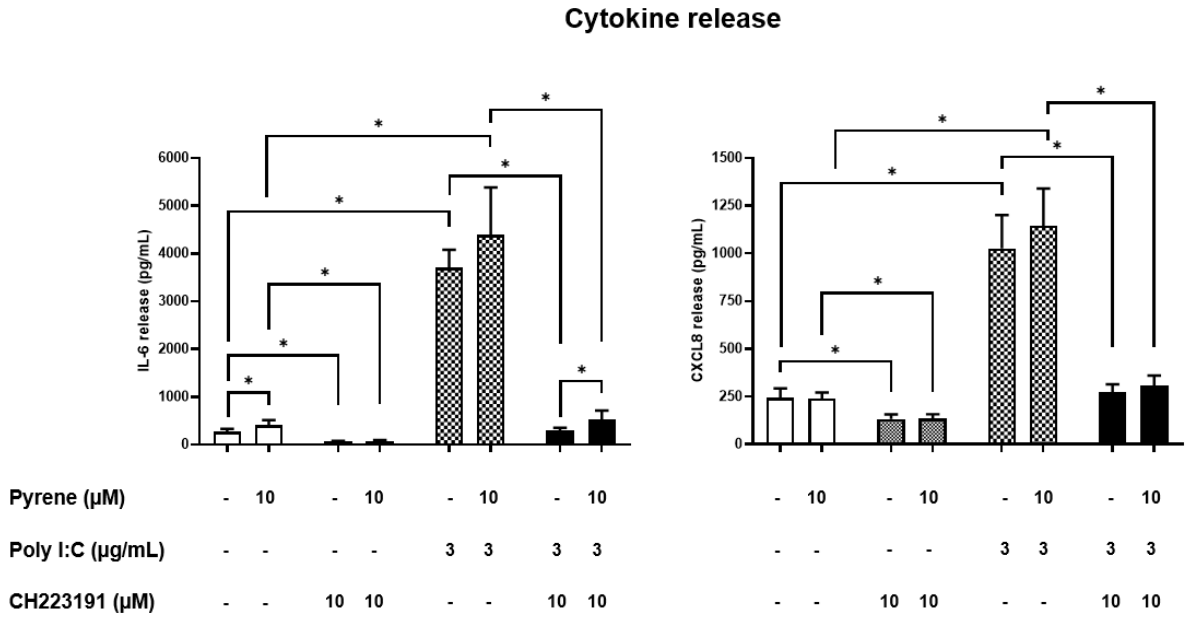

Figure 16 IL-6 and CXCL8 release (pg/mL) after exposing unprimed and primed BEAS-2B cells to pyrene and using the AhR antagonist CH223191. *The cells were primed with Poly I:C (3 µg/mL) and pre-treated with CH223191 (10 µM) for 30 min before 20 h exposure to pyrene (10 µM). The cytokine release was determined by sandwich ELISA. The data are represented as the mean value ± SD of four biological independent replicates with two technical replicates. The results are presented as an increase in IL-6 and CXCL8 release (pg/mL). * is a significant difference between groups (marked with brackets) for Two-way ANOVA with Tukey's multiple comparison test. The statistics were calculated with repeated measures on log-transformed data.*

Next, we examined if the AhR antagonist CH223191 could inhibit the *IL-6* and *CXCL8* expression in unprimed and primed cells. The cells were primed with Poly I:C (3 µg/mL) and treated with CH223191 (10 µM) for 30 min before 5 h exposure to pyrene (1 µM and 10 µM). Four different treatment groups were conducted, as described earlier. Notably, only one experiment with three technical replicates was conducted, and the results only represent the intraexperimental variation (Figure 17).

There was a trend of increasing expression of *IL-6* and *CXCL8* after exposure to 1 µM and 10 µM pyrene. Treating the unprimed cells with CH223191 appeared not to cause a change in *IL-6* and *CXCL8* synthesis when compared to DMSO and pyrene alone. Priming the cells seemed to increase both *IL-6* and *CXCL8* synthesis. Furthermore, pyrene appeared to increase the synthesis in primed cells, whereas exposure to CH223191 in the primed cells seemed to reduce *IL-6* and *CXCL8* expression.

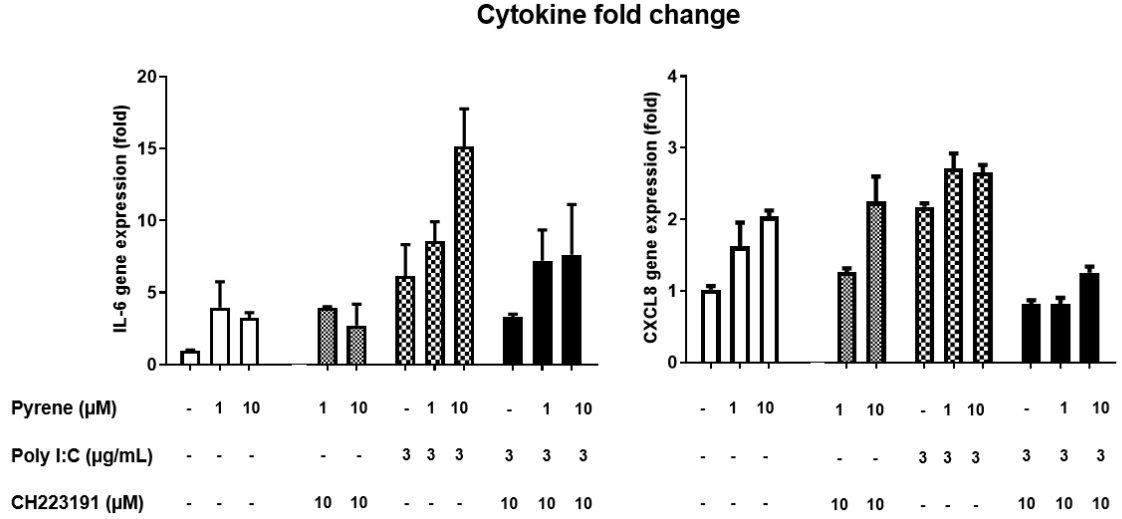

Figure 17 IL-6 and CXCL8 expression after exposing unprimed and primed BEAS-2B cells with pyrene and using the AhR antagonist CH223191. *The cells were primed with Poly I:C (3 µg/mL) and treated with CH223191 (10 µM) for 30 min before 5 h exposure to pyrene (1 µM and 10 µM). The IL-6 and CXCL8 expression was determined by Cell-to-C$_T$. The data are represented as the mean value ± SD of one experiment with three technical replicates of exposure, and results are shown as fold change of the control.*

4.4. Activation of AhR through Ca^{2+}-signaling

Next, we investigated if B[*a*]P and pyrene could activate the non-genomic pathway of AhR by increasing $[Ca^{2+}]_i$. The cells were loaded with a Cal-520 AM dye solution, and fluorescence (RFU) was measured instantly after exposure to the different concentrations (1, 3, and 10 μM) of B[*a*]P and pyrene. Also, two negative controls were conducted, one negative DMSO control and a negative control only containing HHBS buffer.

As seen in the results presented in Figure 18, a minor trend of increase in fluorescence could be observed after exposure to DMSO and all the concentrations of pyrene after 100 min. Similarly, B[*a*]P appeared to slightly increase fluorescence, starting at 100 min. However, as judged from the AUC values (Figure 19), there were no marked changes, nor statistically significant differences between DMSO, pyrene, and B[*a*]P when compared to cells added just HHBS buffer.

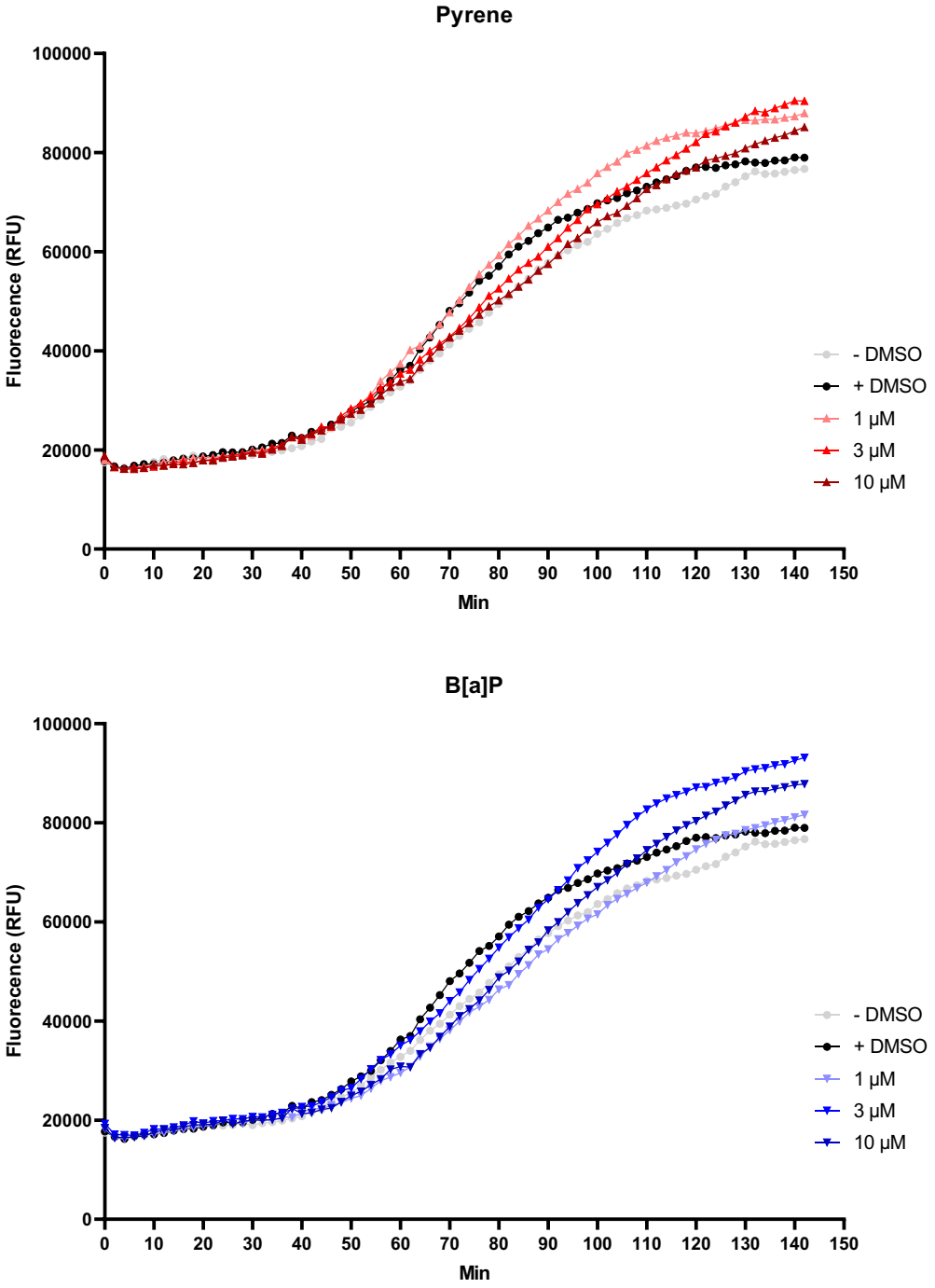

Figure 18 Ca^{2+} release as fluorescence (RFU) levels after exposing BEAS-2B cells to B[a]P and pyrene. *The cells were exposed to B[a]P (1, 3, and 10 µM), and pyrene (1, 3, and 10 µM). The Ca^{2+} levels were determined by measuring fluorescence using Cal-520 AM. The data are represented as the mean value of three biologically independent replicates with four technical replicates. The results are shown as fluorescence (RFU) levels.*

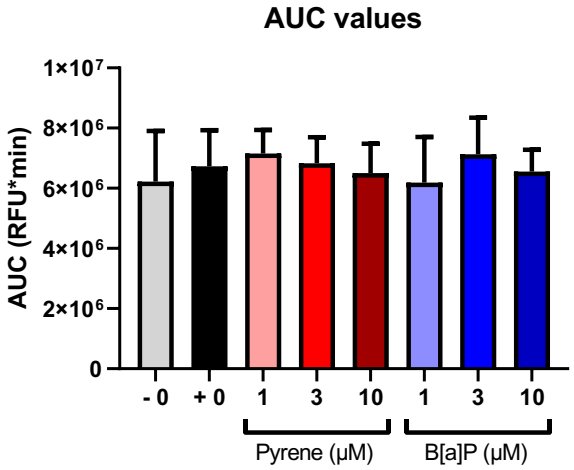

Figure 19 AUC values (RFU*min) of the results presented in Figure 18. *The AUC values were calculated using GraphPad Prism v.8. The results are represented as the mean value ± SD of three biological independent replicates with four technical replicates. The – 0 represents a double negative control (HHBS), and + 0 represents the negative control (DMSO). No significant difference relative to – 0 (HHBS) for One-way ANOVA with Dunnett's multiple comparison test. The statistics were calculated with repeated measures.*

After the Cal-520 AM measurement, the AlamarBlue assay was conducted to determine the viability after measurement. Fluorescence was measured after 90 min, and the viability (%) was calculated using HHBS as the negative control (blank). As shown in Figure 20, none of the treatments reduced the cells' viability.

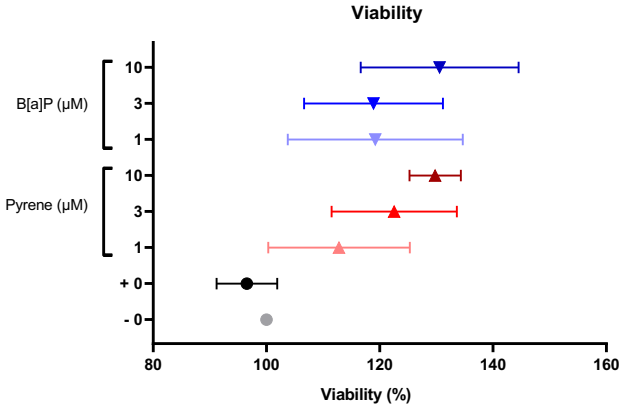

Figure 20 Viability (%) after exposing BEAS-2B cells to pyrene and B[a]P in HHBS buffer. *The cells were exposed to pyrene (1, 3, and 10 μM) and B[a]P (1, 3, and 10 μM) for 142 minutes while measuring Ca^{2+} release. The viability (%) was quantified by using the AlamarBlue assay, using – 0 (HHBS) as blank control. The data are represented as the mean value ± SD of three biologically independent replicates with four technical replicates. No significant difference relative to – 0 (HHBS) for One-way ANOVA with the multiple comparisons Kruskal Wallis test.*

5. Discussion

PAHs are an important part of DPM and have been reported to be an essential driver of pulmonary diseases through inflammatory responses (Totlandsdal, Cassee, Schwarze, Refsnes, & Låg, 2010). In the present thesis, we hypothesized that the various tested PAHs would modify the AhR classical genomic pathway and that AhR activity is essential for the pro-inflammatory responses modulated by the PAHs alone and in combination with the TLR3 ligand Poly I:C. Here we report that the PAHs modulates AhR activity, as measured by increased expression of *CYP1A1*. The antagonistic/agonistic properties towards AhR seemed to be partly dependent on the specific PAH compound and partly the exposure concentration. The various PAHs had none or only marginal effects on IL-6 and no effects on the CXCL8 release in unprimed cells. As for the primed cells, the PAHs impact on cytokine release was somewhat variable, where solely pyrene seemed to have some minor effects on the response. Interestingly, pyrene appeared to increase the synthesis of *IL-6* and *CXCL8* in unprimed and primed cells, which was more marked than the effect seen on cytokine release. When inhibiting AhR activity using the inhibitor CH223191, cytokine release in both unprimed and primed cells, control cells, as well as after exposure to pyrene, were reduced. In contrast, CH223191 did not reduce the synthesis of *IL-6* and *CXCL8* in unprimed cells. Thus, suggesting that the cytokine release is dependent on AhR activity, whereas synthesis in unprimed cells seemed to be independent.

5.1. The PAHs modulates the classical genomic pathway of AhR by modifying *CYP1A1* expression

To exclude the possibility that the modulations in *CYP1A1* expression by the PAHs, was due to a toxic effect, we first checked if any of the compounds alone or in combination had effects on cell death. As judged by both microscopic examination and LDH leakage, none of the PAH exposures at the tested concentrations caused any significant increase in cell death. Notably, the measured max LDH leakage was markedly lower when compared to the other sets of experiments. Thus, indicating that the cell lysis may not have been correctly executed, and our judgment of cytotoxicity is based on the amount of cell leakage of LDH. Thus, the concentration of leaked LDH was not higher compared to the other experiments. These results reassure us that the observed variations in *CYP1A1* expressions, in particular reductions, were not results of cytotoxicity, but more likely effects on the classical genomic pathway of AhR.

To find relevant concentrations for further studies, we decided to make concentration curves of B[*a*]P, a well-known agonist ("Benzo[a]pyrene B01760", n.d.), and pyrene, a possible antagonist of the classical genomic pathway of AhR (Brinchmann et al., 2018). The concentrations used were based on previous findings in our laboratory (Brinchmann et al., 2018). We observed that B[*a*]P seemed to cause a concentration-dependent increase, whereas pyrene appeared to cause a reduction in the *CYP1A1* expression.

Next, we further examined the other PAHs. According to our results, B[*e*]P and phenanthrene seemed to have the highest agonistic effect on AhR. However, 10 µM phenanthrene appeared to cause a slight reduction in expression, indicating possible weak antagonistic properties at higher concentrations. As for the other PAHs (1-MP, fluoranthene, pyrene, 1-NP), a slight, non-significant agonistic effect could be observed at the lowest concentration (0.1 µM). More interesting, non-significant antagonistic effects appeared at higher concentrations (1 µM and 10 µM).

The possible agonistic/antagonistic potential of the various PAHs on the AhR classical genomic pathway was further examined following simultaneous exposure to 0.1 µM B[*a*]P. Importantly, this concentration of B[*a*]P was chosen by being able to give a marked but not fully *CYP1A1* response, as judged by our results. Thus, by using this concentration, it was possible to elucidate

if the PAHs had agonistic or antagonistic effects on the classical genomic pathway of AhR by examining the impact on B[*a*]P-induced *CYP1A1* expression.

Pyrene (0.1 µM and 1 µM) and 1-NP (1 µM) appeared to reduce B[*a*]P-induced *CYP1A1* synthesis; however, only 1 µM 1-NP was statistically significant. These results could indicate that pyrene and 1-NP may mostly have antagonistic properties. In contrast, the other PAHs (phenanthrene, 1-MP, fluoranthene, and B[*e*]P) seemed not to modulate any observable changes in the B[*a*]P-induced *CYP1A1* expression. A trend of reduction in B[*a*]P-induced *CYP1A1* synthesis could be observed after exposure to all the PAHs at the highest concentration (although not significant as tested only twice). Notably, B[*e*]P (10 µM) seemed to cause the smallest reduction in B[*a*]P-induced expression of *CYP1A1*. This could indicate that B[*e*]P is a weak AhR agonist, with lower affinity compared to B[*a*]P, as the latter compound gives effects at lower concentrations and results in a higher response. Overall, these results further indicate that the tested PAHs, except for B[*e*]P, are weak agonists at lower concentrations. Thus, they are not able to reduce B[*a*]P-induced expression but have antagonistic properties at higher concentrations, as observed by a slight, non-significant reduction in B[*a*]P-induced *CYP1A1* synthesis at 10 µM of the PAHs.

The findings presented here are in line with other published results by several other groups. Accordingly, B[*e*]P has been reported to increase *Cyp1a1* expression and EROD activity in rat hepatoma cells (H4IIE) (Houser, Raha, & Vickers, 1992). Also, phenanthrene has been found to activate AhR in a yeast model (YCM3) (Sun, Miller III, Wiese, & Blake, 2014), which may indicate that these two compounds have agonistic properties towards AhR by possibly increasing *CYP1A1* synthesis. In contrast, pyrene has been reported not to alter *Cyp1a1* synthesis nor EROD activity in rat hepatocytes (Till, Riebniger, Schmitz, & Schrenk, 1999; van Meteren et al., 2019). Likewise, Iwanari and coworkers found that pyrene, as well as 1-NP, did not increase *CYP1A1* expression in human lung adenocarcinoma cells (A549) (Iwanari, Nakajima, Kizu, Hayakawa, & Yokoi, 2002). This is in line with our results, suggesting that both pyrene and 1-NP have antagonistic properties towards AhR. Others have reported that fluoranthene does not change the expression of *CYP1A1* in A549 cells and mouse macrophages (RAW264.7) (Iwanari et al., 2002; Wang et al., 2017), nor increase EROD activity in human liver slices (Pushparajah et al., 2008). These results suggest possible antagonistic properties towards AhR by decreasing *CYP1A1* synthesis. However, these findings are only partly

supported by our results, since a slight agonistic effect could be observed at the lowest concentration.

A few other studies have examined AhR activity induced by B[*a*]P in combination with other PAHs. Accordingly, pyrene has been reported to decrease B[*a*]P-induced EROD activity in rats (SIc:SD) (Kang, Jeong, Cho, & Cho, 2007), and 1-NP has been found to reduce B[*a*]P-induced *Cyp1a1* expression in mouse liver cells (Hepa-1c1c7) (Chu et al., 2009). These findings are supported by our results, indicating that 1-NP and pyrene have antagonistic properties towards AhR.

Other groups have, in contrast, published other findings that are not supported by our results. For instance, it has been reported that 1-MP activates the classical genomic pathway of AhR in a yeast model (YCM3) (Sun et al., 2014), and increases *CYP1A1* expression in human liver slices (Pushparajah et al., 2008). This, in contrast to our study, indicates that 1-MP acquire agonistic properties towards AhR. Others have reported that 1-NP increases *CYP1A1* expression and protein production in Hepa-1c1c7 cells (Chu et al., 2009), implying agonistic properties. In contrast, our results instead indicated antagonistic properties towards AhR. Other studies have found that phenanthrene has a low binding affinity to AhR in H4IIE cells (Piskorska-Pliszczynska, Keys, Safe, & Newman, 1986) and does not induce *CYP1A1* expression nor protein production in monocytes (U937) (Ranjit et al., 2016). These findings may imply that phenanthrene has antagonistic properties, which is only partly supported by our results, as the lower concentrations tested seemed to have slight agonistic properties towards AhR.

It is often reported that the larger PAHs, consisting of five benzene rings, have the highest binding potency towards AhR, and may increase *CYP1A1* expression and induce corresponding EROD activity. In contrast, PAHs composed of 2 – 4 benzene rings have lower binding potency and seem to fail (Bosveld, de Bie, Van den Brink, Jongepier, & Klomp, 2002). Our results appear to support these findings partly since phenanthrene, a three-ringed PAH, slightly increased *CYP1A1* expression. Thus, elucidating that there are also other properties of the PAHs important for how strongly they bind to AhR and modulate the expression of genes. Notably, it has previously been found that fluoranthene, pyrene, and B[*e*]P have a weak binding affinity to AhR in HII4E cells (Machala, Vondráček, Bláha, Ciganek, & Neča, 2001), which could indicate

weak agonistic or possibly antagonistic effects or both towards AhR. As seen from our results, it seems like the concentration could be of importance for activating the classical genomic pathway of AhR. Also, it has been reported that the molecular weight may be of importance (Murahashi, Watanabe, Kanayama, Kubo, & Hirayama, 2007).

Various studies seem to report mixed results for the *CYP1A1* expression after exposure to the tested PAHs. Observed disparities could be due to organ/species-specific differences. The experimental setup or differences in exposure times between studies may also explain the observed discrepancy. Notably, the technique used in the current study only measures the amount of mRNA at one specific time point, which does not exclude that changes in the expression could be lower or higher at other exposure durations.

In conclusion, B[*a*]P is a potent AhR agonist, and B[*e*]P and phenanthrene are weak agonists, where the latter compound is an antagonist at higher concentrations. In contrast, 1-MP, fluoranthene, pyrene, and 1-NP are possibly weak agonists at low concentrations, but importantly antagonists at higher concentrations, where the latter two compounds seem to have the highest antagonistic potential. Notably, our results do not exclude the possibility of these PAHs being weak agonists at lower concentrations, which has not been tested.

5.2. The PAHs regulates the cytokine release

Pyrene has been tested the most in our laboratory (Øvrevik et al., 2013); therefore, we decided to do a concentration curve of pyrene alone and in combination with Poly I:C to assess which concentration should be further tested for the other PAHs.

We first checked if any of the concentrations of pyrene had effects on cell death, both in unprimed and primed cells. As judged by both LDH leakage and microscopic examination, there seemed to be no notable increase in cytotoxicity. The primed cells, with or without pyrene, only caused slightly higher cytotoxicity (7-9%) when compared to the unprimed cells (3-5%). These results suggest that cytotoxicity likely had an insignificant effect on the cytokine release.

For the IL-6 release, our results indicate that pyrene induced a concentration-dependent increase in both primed and unprimed cells. However, significant effects were only seen at the higher concentration(s), and the observed increase was minor. For the release of CXCL8, pyrene did

not affect the response in unprimed cells. In contrast, a concentration-dependent increase was observed in primed cells, where 30 μM pyrene caused a significant increase in the release.

Nonetheless, because of higher biological relevance, we decided to examine 10 μM of the other PAHs. Thus, we also checked if 10 μM of the PAHs in unprimed and primed cells caused toxic effects. As seen earlier, a slight significant increase after PAH exposure was seen in the primed cells when compared to the unprimed cells. However, all treatments appeared to cause less than 10% cytotoxicity, indicating that toxic effects should not influence the observed outcome in cytokine release.

For the unprimed cells, we here found that both B[*a*]P and β-NF significantly increased IL-6 release, whereas the other PAHs caused minor or non-observable changes. Notably, pyrene, which caused a small, but significant increase in the first series of experiments, did not significantly increase IL-6 release in this series of experiments, suggesting that the observed effects on IL-6 release are variable. As for the CXCL8 release, β-NF induced a significant increase in the unprimed cells. In contrast, 1-NP marginally but significantly decreased the CXCL8 release. Whereas, the other PAHs did not markedly change the CXCL8 levels. Overall, our results suggest that the PAHs have minimal effects on the IL-6 and CXCL8 response in BEAS-2B cells.

Several groups have tested and published the effects of PAHs on cytokine responses, and the BEAS-2B cells have mostly been used. Accordingly, pyrene has been found to increase the IL-6 response (Koike, Yanagisawa, & Takano, 2014), but not the CXCL8 release (Øvrevik et al., 2013). Our results support these findings since we observed that pyrene was able to induce an increase in the IL-6 response, but in contrast, did not cause any observable change in the CXCL8 release. Interestingly, 1-NP has been reported to decrease the CXCL8 response (Koike et al., 2014), as supported by our results, since a slight significant reduction was observed. As seen in the present study, B[*a*]P has also previously been found not to change the CXCL8 release (Øvrevik et al., 2013). Other studies have used other cell lines; for instance, Ueng and coworkers reported that B[*a*]P increased IL-6 release in human lung adenocarcinoma cells (CL5) (Ueng et al., 2005). Our results support these findings since B[*a*]P was observed to increase IL-6 and not CXCL8 release.

Other groups have published other findings, which are in disagreement with our results. Also, many of these studies have used BEAS-2B cells. For instance, exposure to 1-NP has been reported to increase IL-6 release (Koike et al., 2014), and CXCL8 responses (Øvrevik et al., 2010). In contrast, 1-NP in our results instead caused a marginal reduction in IL-6 and a significant decrease in the CXCL8 release. B[*a*]P has been found not to modify IL-6 responses (Ueng et al., 2005), whereas we observed a significant increase. Øvrevik and coworkers reported that β-NF did not change the CXCL8 release (Øvrevik et al., 2013); in contrast, a significant increase was observed in our results. Other studies have used different experimental models and cell lines. As examples of such studies, fluoranthene has recently been found to increase IL-6 release in RAW264.7 macrophages (Wang et al., 2017). Also, phenanthrene has been reported to increase IL-6 expression and protein production in female rats (Ma et al., 2020). These findings are in contrast to our study, where both fluoranthene and phenanthrene caused no observable change in IL-6 release.

Next, we primed the cells with Poly I:C to assess if pre-existing inflammation would affect the cells' cytokine response towards PAH exposure. As expected, we found that primed cells had a significant increase in IL-6 and CXCL8 release compared to unprimed cells. This illustrates that the presence of viral infection will increase the pro-inflammatory response.

According to earlier findings in our laboratory, both 1-NP and pyrene can increase the CXCL8 release in Poly I:C primed BEAS-2B cells (Øvrevik et al., 2013). Notably, we only observed a slight increase after pyrene exposure, whereas 1-NP caused no observable change. We also observed a significant but marginal increase after exposure to fluoranthene. It also appeared like the cytokine response after PAH exposure in Poly I:C primed cells varied markedly between experiments, and the effects were hard to reproduce. Thus, pyrene exposure caused high variations in the release of IL-6 between experiments, where one set of experiments had an observable effect, but others did not. Also, 10 μM pyrene did not significantly increase the CXCL8 response in the first set of experiments, whereas, in the next series of experiments, a significant increase was observed. These results suggest that pyrene only have marginal effects on the IL-6 and CXCL8 release in primed cells.

Other studies have reported mixed results for the PAH-induced release of IL-6 and CXCL8 in unprimed cells. The disparities between studies could be explained by organ/species-specific differences. Still, discrepancies could also be observed in the same cell line, which may suggest that differences in the experimental setup, cell number, and sensitivity variations between cell batches may modulate the observed disparities. As for the experiments with Poly I:C primed cells, the amount of conducted research is low. Because of the observed variable results, we tried to investigate if the experimental setup was the cause of the observed variance. Therefore, we changed different factors of the experimental system, such as seeding number, cell confluency, and time at exposure. However, we could not find any clear answer to the observed discrepancies. This may indicate that some other factors are causing the observed disparity. Notably, a known problem for *in vitro* experiments using lipid-soluble compounds, such as PAHs, is precipitation and crystallization in the medium. This may imply that the exposure concentration could, in some instances, not be constant, and may cause discrepancies in observed effects, further modulating interexperimental variations.

Interestingly, we also found disparities in the unprimed and primed cells between our results and experiments accomplished earlier in our laboratory. These discrepancies could be caused by using a lower concentration of the PAHs, where higher concentrations have been used earlier. Also, in the current study, we used 6-well culture dishes, while it has earlier been used 12-well culture dishes. This may modulate different responses because of disparities in cell numbers and the amount of medium in the wells at exposure. It is also worth mentioning that the DMSO concentration used in the current study overall was higher (< 1%), compared to the earlier experiments in our laboratory (< 0.5%). Notably, we did not observe any increased cytotoxicity with higher DMSO concentration. However, this does not exclude the possibility that the well-known anti-oxidative properties of DMSO may modify some of the signaling pathways in the study and further modulate discrepancies between other findings (Sanmartín-Suárez, Soto-Otero, Sánchez-Sellero, & Méndez-Álvarez, 2011).

In conclusion, it seems like the PAHs only modulate IL-6 responses in unprimed cells, whereas the CXCL8 release is kept unchanged; however, observed changes in IL-6 release was minor. It further appears that pyrene can cause an increase in cytokine release in primed cells, but observed effects were minor and variable between experiments. In contrast, the other tested PAHs seem not to change the cytokine response notably.

5.3. The importance of AhR for the cytokine release

We further decided to examine the impact of inhibiting AhR activity by CH223191 on the release of IL-6 and CXCL8 in unprimed and primed cells following exposure to pyrene. Thus, we first examined if the various treatments had effects on cell death. As judged by microscopic examination and LDH leakage, a slight statistically significant increase in LDH leakage was seen after all treatments, except for pyrene exposure alone. Treating unprimed cells with CH223191 or only priming the cells with or without pyrene did not exceed 10% cytotoxicity. These results indicate that toxicity probably does not explain the observed variations in cytokine release and gene expression. For the primed cells treated with CH223191 alone or in combination with pyrene, markedly high toxicity was observed (15-20%), suggesting that we cannot exclude that effects further seen on cytokine release and gene expression for these treatments are not the result of cytotoxicity. Thus, interpreting the results should be made with caution. The high observed toxic effect could be the cause of a high DMSO concentration or because of the complex exposure, which may have induced cellular stress ending in cell death.

Here we found that pyrene increased IL-6, but not CXCL8 release in unprimed cells. CH223191 significantly decreased IL-6 and CXCL8 responses after pyrene exposure, suggesting the importance of AhR-dependent activity for the release of cytokines. Notably, CH223191 also markedly reduced the cytokine response in the negative control treated with DMSO, indicating that AhR activity also is essential for the basal level of cytokine release. As for the primed cells, CH223191 significantly reduced IL-6 and CXCL8 release, both with and without pyrene. This could indicate that the observed cytokine responses induced by Poly I:C may also be dependent on AhR activity. However, this reduction may also be the cause of the observed high toxicity.

We further examined if the AhR-induced gene expression was the cause of the specific variations on cytokine release. In unprimed cells, pyrene appeared to increase gene expression of *IL-6* and *CXCL8*, which seemed not to be reduced in the presence of CH223191, indicating that the synthesis may not be dependent on AhR activity. For the primed cells, it appeared as expression increased, and pyrene caused a marginal increase in the synthesis of *IL-6* and *CXCL8*, whereas CH223191 seemed to cause a reduction in the expression. These results could imply that synthesis induced by Poly I:C priming may be partly dependent on AhR activity. However, the observed high toxicity could also explain the apparent reduction.

Notably, from our results, it seems like CH223191 inhibits IL-6 release more thoroughly than the CXCL8 release. The observed disparity could indicate that these cytokines are at least partly released through different mechanisms, and it could be speculated that IL-6 release is slightly more dependent on AhR activity. As recently found in our laboratory, pyrene gave an AhR-dependent increase in $[Ca^{2+}]_i$ (Brinchmann et al., 2018), indicating the importance of AhR-linked Ca^{2+} responses in the release of cytokines. In line with these findings, available Ca^{2+} is reported to be essential in the CXCL8 release (Longhin, Holme, Gualtieri, Camatini, & Øvrevik, 2018; Øvrevik et al., 2011). Furthermore, the release of IL-6 happens through exocytosis, which also is dependent on Ca^{2+} release (Clapham, 2007). Notably, these findings could also explain the observed reduction of IL-6 and CXCL8 levels in the negative control treated with CH223191.

Interestingly, the observed effect of pyrene in unprimed and primed cells is more apparent in the cytokine expression compared to the release. This could suggest that there are disparities between how much is synthesized and the amount released in response to pyrene exposure. Thus, implying that pyrene may have some inhibitory effect on the cytokine response. Also, it seems like the cytokine release, and not the gene expression is dependent on AhR-linked Ca^{2+} release. Furthermore, our results suggest that pyrene may induce the synthesis of *IL-6* and *CXCL8* through another pathway independent of AhR activity.

In conclusion, it seems like AhR-linked Ca^{2+} release could be essential for the regulation of IL-6 and CXCL8 release in unprimed and primed cells. It further appears like the pyrene-induced expression of *IL-6* and *CXCL8* in unprimed cells is independent of AhR-linked Ca^{2+} release. In the primed cells, it seems like expression and release induced by Poly I:C could be dependent on AhR-linked Ca^{2+} response, but the observed reduction could also be due to toxicity. These findings imply that AhR-linked Ca^{2+} release may not be necessary for the cytokine gene expression but may be important for the cytokine release.

5.4. The role of Ca^{2+} in the non-genomic pathway of AhR

As mentioned, it appears that AhR-dependent Ca^{2+} release could be an essential factor in the cytokine responses modulated by PAH exposure. Thus, we also wanted to examine how pyrene and B[*a*]P may modulate Ca^{2+} release. We examined the metabolic activity of the cells after the measurement to exclude that reduced viability caused the observed variations. Notably, the viability appeared not to be altered, indicating that the cells for a short period are not necessarily affected by the lack of CO_2. However, these results do not exclude the possibility of metabolic activity being reduced during measurement. However, these results indicate that the observed variations are not caused by decreased viability.

Both pyrene and B[*a*]P did not markedly increase Ca^{2+} levels. Our results imply that the measured variations in the Ca^{2+} release could be because of the presence of DMSO and not directly effects by the PAH exposures. Accordingly, as judged by the AUC values, there were no observable variations in Ca^{2+} responses, nor significant differences when compared to HHBS control. Thus, our results do not support earlier findings from our laboratory (Brinchmann et al., 2018), where pyrene has been reported to increase Ca^{2+} release.

Our lack of significant effect may just be due to our experimental method, which only measures fluorescence levels. In contrast, other studies have measured Ca^{2+} release by calcium single-cell microscopic imaging (Brinchmann et al., 2018). The disparities could suggest that the approach in the present study is not sensitive enough for measuring Ca^{2+} release in bronchial epithelial cells. Also, since the HHBS control also seemed to increase fluorescence, this could imply that the lack of CO_2 during measurement may have some effect on the cells' response. Notably, the exposures were accomplished in HHBS buffer not containing protein, which also could cause higher precipitation of the PAHs. Thus, indicating that the exposure might not have been continuous during the entire measurement, and the specific treatments may not have caused the observed increase in fluorescence.

In conclusion, our results suggest that pyrene and B[*a*]P does not increase Ca^{2+} release as measured by fluorescence. However, our results do not exclude that Ca^{2+} release may be of importance for the cells' response to PAHs.

5.5. Limitations and future studies

Our results could indicate that the present experimental system may not be sensitive enough for testing possible pro-inflammatory responses after exposure to the tested PAHs. It would thus have been interesting to examine the PAHs effect on inflammatory responses further using other cell lines, including primary cells, and growing the cells in 3D cultures or by using inserts, which may enhance their sensitivity. Also, it could be interesting to measure *CYP1A1* expression using lower concentrations of the PAHs to assess at which concentrations they have agonistic properties towards AhR. Furthermore, investigating different exposure periods for the gene expression to elucidate which time point has the most effect would be of interest. As for the cytokine release, the variable effects of the PAHs and Poly I:C induced release should be further investigated by altering different experimental factors to assess the mechanism behind the observed variations.

The most exciting result presented in the current study is the apparent difference seen between synthesis and cytokine release after pyrene exposure. These results imply that the release could be somewhat inhibited by pyrene. Thus, the mechanism and signaling pathway behind gene expression induced by PAHs, and the possible inhibitory effects on cytokine release should be further examined. Also, the importance of AhR in these processes and the importance of Ca^{2+} release after PAH exposure using calcium single-cell microscopic imaging, and how this affects cytokine release modulated by the PAHs with or without other various activators of TLR, including Poly I:C, should also be further examined.

6. Conclusion

The results reported in the present study suggest that exposure to the tested PAHs modifies the classical genomic pathway of AhR by altering *CYP1A1* expression. B[*a*]P, B[*e*]P, and phenanthrene have agonistic potential, but the latter compound has antagonistic properties at higher concentrations. We cannot exclude the possibility that the other PAHs tested (1-MP, fluoranthene, pyrene, and 1-NP) may have agonistic potential at lower concentrations; we more clearly demonstrate antagonistic properties towards AhR. In general, the tested PAHs cause none or only marginal effects on IL-6 responses in unprimed cells, whereas the CXCL8 release is unchanged. This is in line with other studies suggesting that different mechanisms may partly modulate the release of these cytokines. In the primed cells, pyrene caused a marginal increase in cytokine release, whereas the other PAHs did not change the response. Pyrene appeared to increase the *IL-6* and *CXCL8* expression, while the release varied in both unprimed and primed cells, suggesting that pyrene stimulates the synthesis but, at the same time, partly inhibits the process of cytokine release. Notably, it seemed like the release but not the synthesis of these cytokines is dependent on an AhR-linked process as judged by the inhibition of AhR using the AhR antagonist CH223191. Pyrene and B[*a*]P did not increase Ca^{2+} release based on measuring fluorescence; however, our lack of effects may be due to using a method with low sensitivity. Overall, we found that the various PAHs, to a certain degree, modulates the AhR activity, but they seem to have marginal effects on pro-inflammatory responses in bronchial epithelial cells.

7. References

"Benzo[a]pyrene B01760". (n.d.). Benzo[a]pyrene B01760. Retrieved 3 August 2020, from https://www.sigmaaldrich.com/catalog/product/sigma/b1760?lang=en&region=NO

"Cal-520® AM". (2017, January 2017). Cal-520®, AM | AAT Bioquest. Retrieved 30 May 2020, from https://www.aatbio.com/products/cal-520-am#jump_protocol

"CH223191". (n.d.). CH223191. Retrieved 4 September 2020, from https://www.sigmaaldrich.com/catalog/product/sigma/c8124?lang=en

"Cytotoxicity Detection Kit (LDH)". (n.d.). Cytotoxicity Detection KitPLUS (LDH) CYTODETRO. Retrieved 18 June 2020, from https://www.sigmaaldrich.com/catalog/product/roche/cytodetro?lang=en&region=NO&cm_sp=Insite-_-caContent_prodMerch_gruCrossEntropy-_-prodMerch10-1

"Primary Cell Culture Basics". (n.d.). Primary Cell Culture Basics. Retrieved 10 July 2020, from https://www.sigmaaldrich.com/technical-documents/articles/biology/primary-cell-culture.html

"Sandwich ELISA protocol". (2019). Sandwich ELISA protocol. Retrieved 15 July 2020, from https://www.leinco.com/sandwich-elisa-protocol/

"SciFinder". (n.d., 2020). SciFinder. Retrieved 4 February 2020, from https://scifinder-n.cas.org/

Aikawa, T., Shimura, S., Sasaki, H., Ebina, M., & Takishima, T. (1992). Marked goblet cell hyperplasia with mucus accumulation in the airways of patients who died of severe acute asthma attack. *Chest, 101*(4), 916-921. doi:10.1378/chest.101.4.916

Alexopoulou, L., Holt, A. C., Medzhitov, R., & Flavell, R. A. (2001). Recognition of double-stranded RNA and activation of NF-κB by toll-like receptor 3. *Nature, 413*(6857), 732-738. doi:10.1038/35099560

Apicella, B., Mancaruso, E., Russo, C., Tregrossi, A., Oliano, M. M., Ciajolo, A., & Vaglieco, B. M. (2020). Effect of after-treatment systems on particulate matter emissions in diesel engine exhaust. *Experimental Thermal and Fluid Science*, 110107. doi:10.1016/j.expthermflusci.2020.110107

Atkinson, R. W., Fuller, G. W., Anderson, H. R., Harrison, R. M., & Armstrong, B. (2010). Urban ambient particle metrics and health: A time-series analysis. *Epidemiology*, 501-511. doi:0.1097/EDE.ObO 13e3181 debc8

Bach, N., Bølling, A. K., Brinchmann, B. C., Totlandsdal, A. I., Skuland, T., Holme, J. A., Låg, M., Schwarze, P. E., & Øvrevik, J. (2015). Cytokine responses induced by diesel exhaust particles are suppressed by PAR-2 silencing and antioxidant treatment, and driven by polar and non-polar soluble constituents. *Toxicology Letters, 238*(2), 72-82. doi:10.1016/j.toxlet.2015.07.002

Baggiolini, M., Walz, A., & Kunkel, S. L. (1989). Neutrophil-activating peptide-1/interleukin 8, a novel cytokine that activates neutrophils. *The Journal of Clinical Investigation, 84*(4), 1045-1049. doi:10.1172/JCI114265

Bonvallot, V., Baeza-Squiban, A., Baulig, A., Brulant, S., Boland, S., Muzeau, F., Barouki, R., & Marano, F. (2001). Organic compounds from diesel exhaust particles elicit a proinflammatory response in human airway epithelial cells and induce cytochrome p450 1A1 expression. *American Journal of Respiratory Cell and Molecular Biology, 25*(4), 515-521. doi:10.1165/ajrcmb.25.4.4515

Boström, C.-E., Gerde, P., Hanberg, A., Jernström, B., Johansson, C., Kyrklund, T., Rannug, A., Törnqvist, M., Victorin, K., & Westerholm, R. (2002). Cancer risk assessment, indicators, and guidelines for polycyclic aromatic hydrocarbons in the ambient air. *Environmental Health Perspectives, 110*(suppl 3), 451-488. doi:10.1289/ehp.110-1241197

Bosveld, A. T., de Bie, P. A., Van den Brink, N. W., Jongepier, H., & Klomp, A. V. (2002). In vitro EROD induction equivalency factors for the 10 PAHs generally monitored in risk assessment studies in the Netherlands. *Chemosphere, 49*(1), 75-83. doi:10.1016/S0045-6535(02)00161-3

Brinchmann, B. C., Le Ferrec, E., Bisson, W. H., Podechard, N., Huitfeldt, H. S., Gallais, I., Sergent, O., Holme, J. A., Lagadic-Gossmann, D., & Øvrevik, J. (2018). Evidence of selective activation of aryl hydrocarbon

receptor nongenomic calcium signaling by pyrene. *Biochemical Pharmacology, 158*(2018), 1-12. doi:10.1016/j.bcp.2018.09.023

Brook, R. D., Franklin, B., Cascio, W., Hong, Y., Howard, G., Lipsett, M., Luepker, R., Mittleman, M., Samet, J., Smith, S. C., & Tager, I. (2004). Air Pollution and cardiovascular disease. *Circulation, 109*(21), 2655-2671. doi:10.1161/01.cir.0000128587.30041.c8

Brunekreef, B., & Holgate, S. T. (2002). Air pollution and health. *The Lancet, 360*(9341), 1233-1242. doi:10.1016/s0140-6736(02)11274-8

Cadelis, G., Tourres, R., & Molinie, J. (2014). Short-term effects of the particulate pollutants contained in Saharan dust on the visits of children to the emergency department due to asthmatic conditions in Guadeloupe (French Archipelago of the Caribbean). *PloS One, 9*(3). doi:10.1371/ journal.pone.0091136

Cao, Y., Chen, M., Dong, D., Xie, S., & Liu, M. (2020). Environmental pollutants damage airway epithelial cell cilia: Implications for the prevention of obstructive lung diseases. *Thoracic Cancer, 11*(2020), 505-510. doi:10.1111/1759-7714.13323

Chu, W.-C., Hong, W.-F., Huang, M.-C., Chen, F.-Y., Lin, S.-C., Liao, P.-J., & Su, J.-G. J. (2009). 1-Nitropyrene stabilizes the mRNA of cytochrome P450 1a1, a carcinogen-metabolizing enzyme, via the Akt pathway. *Chemical Research in Toxicology, 22*(12), 1938-1947. doi:10.1021/tx900241g

Clapham, D. E. (2007). Calcium signaling. *Cell, 131*(6), 1047-1058. doi:10.1016/j.cell.2007.11.028

Courcot, E., Leclerc, J., Lafitte, J.-J., Mensier, E., Jaillard, S., Gosset, P., Shirali, P., Pottier, N., Broly, F., & Lo-Guidice, J.-M. (2012). Xenobiotic metabolism and disposition in human lung cell models: Comparison with in vivo expression profiles. *Drug Metabolism and Disposition, 40*(10), 1953-1965. doi:10.1124/dmd.112.046896

Cruse, G., & Bradding, P. (2016). Mast cells in airway diseases and interstitial lung disease. *European Journal of Pharmacology, 778*, 125-138. doi:10.1016/j.ejphar.2015.04.046

Dat, N.-D., & Chang, M. B. (2017). Review on characteristics of PAHs in atmosphere, anthropogenic sources and control technologies. *Science of The Total Environment, 609*, 682-693. doi:10.1016/j.scitotenv.2017.07.204

Donaldson, K., Stone, V., Borm, P. J. A., Jimenez, L. A., Gilmour, P. S., Schins, R. P. F., Knaapen, A. M., Rahman, I., Faux, S. P., Brown, D. M., & Macnee, W. (2003). Oxidative stress and calcium signaling in the adverse effects of environmental particles (PM10). *Free Radical Biology and Medicine, 34*(11), 1369-1382. doi:10.1016/s0891-5849(03)00150-3

Downey, G. P., Worthen, G. S., Henson, P. M., & Hyde, D. M. (1993). Neutrophil sequestration and migration in localized pulmonary inflammation. *The American Review of Respiratory Disease, 147*(1), 168-176. doi:10.1164/ajrccm/147.1.168

Dunnett, C. W. (1955). A multiple comparison procedure for comparing several treatments with a control. *Journal of the American Statistical Association, 50*(272), 1096-1121. doi:10.1080/01621459.1955.10501294

Durant, J. L., Busby, W. F., Lafleur, A. L., Penman, B. W., & Crespi, C. L. (1996). Human cell mutagenicity of oxygenated, nitrated and unsubstituted polycyclic aromatic hydrocarbons associated with urban aerosols. *Genetic Toxicology, 371*(3-4), 123-157. doi:10.1016/s0165-1218(96)90103-2

Esworthy, R. (2013). *Air quality: EPA's 2013 Changes to the Particulate Matter (PM) Standard*. Retrieved from https://www.everycrsreport.com/files/20150107_R42934_1ff9cb6b83e567019f30f3f101475a68264fddbd.pdf

Gamaley, I. A., & Klyubin, I. V. (1999). Roles of reactive oxygen species: Signaling and regulation of cellular functions. *International Review of Cytology, 188*. doi:10.1016/S0074-7696(08)61568-5

Gomperts, B. D., Kramer, I. M., & Tatham, P. E. R. (2009a). First Messengers. In *Signal Transduction* (2nd ed., pp. 21-45). ISBN: 978-0-12-369441-6

Gomperts, B. D., Kramer, I. M., & Tatham, P. E. R. (2009b). Prologue: Signal Transduction, Origins, Ancestors. In *Signal Transduction* (2nd ed., pp. 1-20). ISBN: 978-0-12-369441-6

Holme, J. A., Brinchmann, B. C., Le Ferrec, E., Lagadic-Gossmann, D., & Øvrevik, J. (2019). Combustion particle-induced changes in calcium homeostasis: A contributing factor to vascular disease? *Cardiovascular Toxicology, 19*(3), 198-209. doi:10.1007/s12012-019-09518-9

Houser, W. H., Raha, A., & Vickers, M. (1992). Induction of CYP1A1 gene expression in H4-II-E rat hepatoma cells by benzo [e] pyrene. *Molecular Carcinogenesis, 5*(3), 232-237. doi:10.1002/mc.2940050310

IARC. (2010). *Some Non-heterocyclic Polycyclic Aromatic Hydrocarbons and Some Related Exposures* (Vol. 92). Lyon, France: International Agency for Research on Cancer. ISBN: 978-92-832-1292-8

IARC. (2014). *Diesel and Gasoline Engine Exhausts and Some Nitroarenes* (Vol. 105). Lyon, France: International Agency for Research on Cancer. ISBN: 978-92-832-0143-4

IARC. (2017). *Air Pollution and Cancer*: International Agency for Research on Cancer ISBN: 978-92-832-2166-1

Iwanari, M., Nakajima, M., Kizu, R., Hayakawa, K., & Yokoi, T. (2002). Induction of CYP1A1, CYP1A2, and CYP1B1 mRNAs by nitropolycyclic aromatic hydrocarbons in various human tissue-derived cells: Chemical-, cytochrome P450 isoform-, and cell-specific differences. *Archives of Toxicology, 76*(5-6), 287-298. doi:10.1007/s00204-002-0340-z

Jin, Y., Zhu, M., Guo, Y., Foreman, D., Feng, F., Duan, G., Wu, W., & Zhang, W. (2019). Fine particulate matter (PM2.5) enhances FcεRI-mediated signaling and mast cell function. *Cellular Signaling, 57*, 102-109. doi:10.1016/j.cellsig.2019.01.010

Kampa, M., & Castanas, E. (2008). Human health effects of air pollution. *Environmental Pollution, 151*(2), 362-367. doi:10.1016/j.envpol.2007.06.012

Kang, H. G., Jeong, S. H., Cho, M. H., & Cho, J. H. (2007). Changes of biomarkers with oral exposure to benzo (a) pyrene, phenanthrene and pyrene in rats. *Journal of Veterinary Science, 8*(4), 361-368. doi:10.4142/jvs.2007.8.4.361

Kelly, F. J., & Fussell, J. C. (2012). Size, source and chemical composition as determinants of toxicity attributable to ambient particulate matter. *Atmospheric Environment, 60*, 504-526. doi:10.1016/j.atmosenv.2012.06.039

Kim, K.-H., Jahan, S. A., Kabir, E., & Brown, R. J. (2013). A review of airborne polycyclic aromatic hydrocarbons (PAHs) and their human health effects. *Environment International, 60*, 71-80. doi:10.1016/j.envint.2013.07.019

Kim, Y.-D., Ko, Y.-J., Kawamoto, T., & Kim, H. (2005). The effects of 1-Nitropyrene on oxidative DNA damage and expression of DNA repair enzymes. *Journal of Occupational Health, 47*(3), 261-266. doi:10.1539/joh.47.261

Koike, E., Yanagisawa, R., & Takano, H. (2014). Toxicological effects of polycyclic aromatic hydrocarbons and their derivatives on respiratory cells. *Atmospheric Environment, 97*, 529-536. doi:10.1016/j.atmosenv.2014.04.003

Kroemer, G., Galluzzi, L., Vandenabeele, P., Abrams, J., Alnemri, E. S., Baehrecke, E. H., Blagosklonny, M. V., El-Deiry, W. S., Golstein, P., Green, D. R., Hengartner, M., Knight, R. A., Kumar, S., Lipton, S. A., Malorni, W., Nuñez, G., Peter, M. E., Tschopp, J., Yuan, J., Piacentini, M., Zhivotovsky, B., & Melino, G. (2009). Classification of cell death: Recommendations of the Nomenclature Committee on Cell Death 2009. *Cell Death and Differentiation, 16*(1), 3-11. doi:10.1038/cdd.2008.150

Lafferty, E. I., Qureshi, S. T., & Schnare, M. (2010). The role of toll-like receptors in acute and chronic lung inflammation. *Journal of Inflammation, 7*(1), 57. doi:10.1186/1476-9255-7-57

Landrigan, P. J., Fuller, R., Acosta, N. J., Adeyi, O., Arnold, R., Baldé, A. B., Bertollini, R., Bose-O'Reilly, S., Boufford, J. I., & Breysse, P. N. (2018). The Lancet Commission on pollution and health. *The Lancet, 391*(10119), 462-512. doi:10.1016/S0140-6736(17)32345-0

Lannerö, E., Wickman, M., van Hage, M., Bergström, A., Pershagen, G., & Nordvall, L. (2008). Exposure to environmental tobacco smoke and sensitisation in children. *Thorax, 63*(2), 172-176. doi:10.1136/thx.2007.079053

Leng, S. X., McElhaney, J. E., Walston, J. D., Xie, D., Fedarko, N. S., & Kuchel, G. A. (2008). ELISA and multiplex technologies for cytokine measurement in inflammation and aging research. *The Journals of Gerontology Series A: Biological Sciences and Medical Sciences, 63*(8), 879-884. doi:10.1093/gerona/63.8.879

Lenner, M., & Karlsson, B. O. (1998). *Quantitative calculation model for the emissions of carcinogenic pollutants by traffic in Swedish urban areas* (0347—6049). Retrieved from http://worldcat.org/issn/03476049

Lock, J. T., Parker, I., & Smith, I. F. (2015). A comparison of fluorescent Ca2+ indicators for imaging local Ca2+ signals in cultured cells. *Cell Calcium, 58*(6), 638-648. doi:10.1016/j.ceca.2015.10.003

Löndahl, J., Massling, A., Pagels, J., Swietlicki, E., Vaclavik, E., & Loft, S. (2007). Size-resolved respiratory-tract deposition of fine and ultrafine hydrophobic and hygroscopic aerosol particles during rest and exercise. *Inhalation Toxicology, 19*(2), 109-116. doi:10.1080/08958370601051677

Longhin, E., Holme, J. A., Gualtieri, M., Camatini, M., & Øvrevik, J. (2018). Milan winter fine particulate matter (wPM2. 5) induces IL-6 and IL-8 synthesis in human bronchial BEAS-2B cells, but specifically impairs IL-8 release. *Toxicology in Vitro, 52*, 365-373. doi:10.1016/j.tiv.2018.07.016

Ma, H., Wang, H., Zhang, H., Guo, H., Zhang, W., Hu, F., Yao, Y., Wang, D., Li, C., & Wang, J. (2020). Effects of phenanthrene on oxidative stress and inflammation in lung and liver of female rats. *Environmental Toxicology, 35*(1), 37-46. doi:10.1002/tox.22840

Machala, M., Vondráček, J., Bláha, L., Ciganek, M., & Neča, J. (2001). Aryl hydrocarbon receptor-mediated activity of mutagenic polycyclic aromatic hydrocarbons determined using in vitro reporter gene assay. *Mutation Research/Genetic Toxicology and Environmental Mutagenesis, 497*(1-2), 49-62. doi:10.1016/S1383-5718(01)00240-6

Matsumura, F. (2009). The significance of the nongenomic pathway in mediating inflammatory signaling of the dioxin-activated Ah receptor to cause toxic effects. *Biochemical Pharmacology, 77*(4), 608-626. doi:10.1016/j.bcp.2008.10.013

Mills, P. R., Davies, R. J., & Devalia, J. L. (1999). Airway epithelial cells, cytokines, and pollutants. *American Journal of Respiratory and Critical Care Medicine, 160*, S38-S43. doi:10.1164/ajrccm.160.supplement_1.11

Miyata, R., & van Eeden, S. F. (2011). The innate and adaptive immune response induced by alveolar macrophages exposed to ambient particulate matter. *Toxicology and Applied Pharmacology, 257*(2), 209-226. doi:10.1016/j.taap.2011.09.007

Mizel, S. B. (1989). The interleukins 1. *The FASEB Journal, 3*(12), 2379-2388. doi:10.1096/fasebj.3.12.2676681

Murahashi, T., Watanabe, T., Kanayama, M., Kubo, T., & Hirayama, T. (2007). Human aryl hydrocarbon receptor ligand activity of 31 non-substituted polycyclic aromatic hydrocarbons as soil contaminants. *Journal of Health Science, 53*(6), 715-721. doi:10.1248/jhs.53.715

Murphy, K., & Weaver, C. (2017a). Basic Concepts in Immunology. In *Janeway's Immunobiology* (9th ed., pp. 1-24). ISBN: 978-0-8153-4505-3

Murphy, K., & Weaver, C. (2017b). The Induced Response of Innate Immunity. In *Janeway's Immunobiology* (9th ed., pp. 77-132). ISBN: 978-0-8153-4505-3

Namazi, M. R. (2009). Cytochrome-P450 enzymes and autoimmunity: Expansion of the relationship and introduction of free radicals as the link. *Journal of Autoimmune Diseases, 6*(1). doi:10.1186/1740-2557-6-4

Nowakowski, M., Rostkowski, P., & Andrzejewski, P. (2017). *Oxidized forms of polycyclic aromatic hydrocarbons (Oxy-PAHs): determination in suspended particulate matter (SPM).* Paper presented at the 15th International Conference on Environmental Science and Technology, Rhodes, Greece.

Olsson, A. C., Fevotte, J., Fletcher, T., Cassidy, A., Mannetje, A. t., Zaridze, D., Szeszenia-Dabrowska, N., Rudnai, P., Lissowska, J., & Fabianova, E. (2010). Occupational exposure to polycyclic aromatic hydrocarbons and lung cancer risk: A multicenter study in Europe. *Occupational and Environmental Medicine, 67*(2), 98-103. doi:10.1136/oem.2009.046680

Oswald, N. (2019, 16 July). What is a Cq (Ct) Value? Retrieved 20 June 2020, from https://bitesizebio.com/24581/what-is-a-ct-value/

Parham, P. (2015a). Elements of the Immune System and their Roles in Defense. In *The Immune System* (4th ed., pp. 1-27). ISBN: 9780815345268

Parham, P. (2015b). Innate Immunity: The Induced Response to Infection. In *The Immune System* (4th ed., pp. 47-78). ISBN: 9780815345268

Park, E.-J., & Park, K. (2009). Induction of pro-inflammatory signals by 1-nitropyrene in cultured BEAS-2B cells. *Toxicology Letters, 184*(2), 126-133. doi:10.1016/j.toxlet.2008.10.028

Pfeffer, P. E., Ho, T. R., Mann, E. H., Kelly, F. J., Sehlstedt, M., Pourazar, J., Dove, R. E., Sandstrom, T., Mudway, I. S., & Hawrylowicz, C. M. (2018). Urban particulate matter stimulation of human dendritic cells enhances priming of naive CD 8 T lymphocytes. *Immunology, 153*(4), 502-512. doi:10.1111/imm.12852

Piskorska-Pliszczynska, J., Keys, B., Safe, S., & Newman, M. (1986). The cytosolic receptor binding affinities and AHH induction potencies of 29 polynuclear aromatic hydrocarbons. *Toxicology Letters, 34*(1), 67-74. doi:10.1016/0378-4274(86)90146-3

Proud, D., & Leigh, R. (2011). Epithelial cells and airway diseases. *Immunological Reviews, 242*(1), 186-204. doi:10.1111/j.1600-065x.2011.01033.x

Prüss-Ustün, A., Vickers, C., Haefliger, P., & Bertollini, R. (2011). Knowns and unknowns on burden of disease due to chemicals: A systematic review. *Environmental Health, 10*(1), 9. doi:10.1186/1476-069X-10-9

Pushparajah, D. S., Umachandran, M., Nazir, T., Plant, K. E., Plant, N., Lewis, D. F., & Ioannides, C. (2008). Up-regulation of CYP1A/B in rat lung and liver, and human liver precision-cut slices by a series of polycyclic aromatic hydrocarbons; association with the Ah locus and importance of molecular size. *Toxicology in Vitro, 22*(1), 128-145. doi:10.1016/j.tiv.2007.08.014

Quay, J. L., Reed, W., Samet, J., & Devlin, R. B. (1998). Air pollution particles induce IL-6 gene expression in human airway epithelial cells via NF-κ B activation. *American Journal of Respiratory Cell and Molecular Biology, 19*(1), 98-106. doi:10.1165/ajrcmb.19.1.3132

Ranjit, S., Midde, N. M., Sinha, N., Patters, B. J., Rahman, M. A., Cory, T. J., Rao, P., & Kumar, S. (2016). Effect of polyaryl hydrocarbons on cytotoxicity in monocytic cells: Potential role of cytochromes P450 and oxidative stress pathways. *PloS One, 11*(9). doi:10.1371/journal.pone.0163827

Ristovski, Z. D., Miljevic, B., Surawski, N. C., Morawska, L., Fong, K. M., Goh, F., & Yang, I. A. (2012). Respiratory health effects of diesel particulate matter. *Respirology, 17*(2), 201-212. doi:10.1111/j.1440-1843.2011.02109.x

Sanmartín-Suárez, C., Soto-Otero, R., Sánchez-Sellero, I., & Méndez-Álvarez, E. (2011). Antioxidant properties of dimethyl sulfoxide and its viability as a solvent in the evaluation of neuroprotective antioxidants. *Journal of Pharmacological and Toxicological Methods, 63*(2), 209-215. doi:10.1016/j.vascn.2010.10.004

Schindler, R., Mancilla, J., Endres, S., Ghorbani, R., Clark, S., & Dinarello, C. A. (1990). Correlations and interactions in the production of interleukin-6 (IL-6), IL-1, and tumor necrosis factor (TNF) in human blood mononuclear cells: IL-6 suppresses IL-1 and TNF. *Blood, 75*(1), 40-47. doi:10.1182/blood.V75.1.40.40

Schlesinger, R. B., & Lippmann, M. (1978). Selective particle deposition and bronchogenic carcinoma. *Environmental Research, 15*(3), 424-431. doi:10.1016/0013-9351(78)90123-8

Schreck, R., & Baeuerle, P. A. (1991). A role for oxygen radicals as second messengers. *Trends in Cell Biology, 1*(2-3), 39-42. doi:10.1016/0962-8924(91)90072-h

Schreck, R., Rieber, P., & Baeuerle, P. A. (1991). Reactive oxygen intermediates as apparently widely used messengers in the activation of the NF-kappa B transcription factor and HIV-1. *The EMBO Journal, 10*(8), 2247-2258. doi:10.1002/j.1460-2075.1991.tb07761.x

Schwarze, P. E., Øvrevik, J., Låg, M., Refsnes, M., Nafstad, P., Hetland, R. B., & Dybing, E. (2006). Particulate matter properties and health effects: Consistency of epidemiological and toxicological studies. *Human & Experimental Toxicology, 25*(10), 559-579. doi:10.1177/096032706072520

Simon, H.-U., Haj-Yehia, A., & Levi-Schaffer, F. (2000). Role of reactive oxygen species (ROS) in apoptosis induction. *Apoptosis, 5*(5), 415-418. doi:10.1023/a:1009616228304

Smart, R. C., & Hodgson, E. (2018). Structure, Mechanism, and Regulation of Cytochrome P450. In *Molecular and Biochemical Toxicology* (5th ed., pp. 209-238). ISBN: 9781119042419

Sun, Y., Miller III, C. A., Wiese, T. E., & Blake, D. A. (2014). Methylated phenanthrenes are more potent than phenanthrene in a bioassay of human aryl hydrocarbon receptor (AhR) signaling. *Environmental Toxicology and Chemistry, 33*(10), 2363-2367. doi:10.1002/etc.2687

Tekpli, X., Holme, J. A., Sergent, O., & Lagadic-Gossmann, D. (2013). Role for membrane remodeling in cell death: Implication for health and disease. *Toxicology, 304*, 141-157. doi:10.1016/j.tox.2012.12.014

Tian, Y., Rabson, A. B., & Gallo, M. A. (2002). Ah receptor and NF-κB interactions: Mechanisms and physiological implications. *Chemico-Biological Interactions, 141*(1-2), 97-115. doi:10.1016/s0009-2797(02)00068-6

Tietz, N. W. (1985). *Textbook of Clinical Chemistry* (1st ed.). ISBN: 0721688861

Till, M., Riebniger, D., Schmitz, H.-J., & Schrenk, D. (1999). Potency of various polycyclic aromatic hydrocarbons as inducers of CYP1A1 in rat hepatocyte cultures. *Chemico-Biological Interactions, 117*(2), 135-150. doi:10.1016/S0009-2797(98)00105-7

Timbrell, J. A. (2009). Factors Affecting Metabolism and Disposition. In *Principles of Biochemical Toxicology* (4th ed., pp. 170-180). ISBN: 978-0-8493-7302-2

Tokiwa, H., Sera, N., Horikawa, K., Nakanishi, Y., & Shigematu, N. (1993). The presence of mutagens/carcinogens in the excised lung and analysis of lung cancer induction. *Carcinogenesis, 14*(9), 1933-1938. doi:10.1093/carcin/14.9.1933

Totlandsdal, A. I., Cassee, F. R., Schwarze, P., Refsnes, M., & Låg, M. (2010). Diesel exhaust particles induce CYP1A1 and pro-inflammatory responses via differential pathways in human bronchial epithelial cells. *Particle and Fibre Toxicology, 7*(1), 41. doi:10.1186/1743-8977-7-41

Tukey, J. W. (1949). Comparing individual means in the analysis of variance. *Biometrics, 5*(2), 99-114. doi:10.2307/3001913

Ueng, T.-H., Hung, C.-C., Kuo, M.-L., Chan, P.-K., Hu, S.-H., Yang, P.-C., & Chang, L. W. (2005). Induction of fibroblast growth factor-9 and interleukin-1α gene expression by motorcycle exhaust particulate extracts and benzo (a) pyrene in human lung adenocarcinoma cells. *Toxicological Sciences, 87*(2), 483-496. doi:10.1093/toxsci/kfi251

van Meteren, N., Lagadic-Gossmann, D., Chevanne, M., Gallais, I., Gobart, D., Burel, A., Bucher, S., Grova, N., Fromenty, B., & Appenzeller, B. M. (2019). Polycyclic aromatic hydrocarbons can trigger hepatocyte release of extracellular vesicles by various mechanisms of action depending on their affinity for the aryl hydrocarbon receptor. *Toxicological Sciences, 171*(2), 443-462. doi:10.1093/toxsci/kfz157

Wang, C., Yang, J., Zhu, L., Yan, L., Lu, D., Zhang, Q., Zhao, M., & Li, Z. (2017). Never deem lightly the "less harmful" low-molecular-weight PAH, NPAH, and OPAH — Disturbance of the immune response at real environmental levels. *Chemosphere, 168*, 568-577. doi:10.1016/j.chemosphere.2016.11.024

Waugh, A., & Grant, A. (2014). The Respiratory System. In *Ross and Wilson Anatomy & Physiology in Health and Illness* (12th ed., pp. 243-270). ISBN: 978-0-7020-5326-9

Whitlock Jr, J. P. (1999). Induction of cytochrome P4501A1. *Annual Review of Pharmacology and Toxicology, 39*(1), 103-125. doi:10.1146/annurev.pharmtox.39.1.103

Whitlock, M. C., & Schluter, D. (2015a). Comparing Two Means. In *The Analysis of Biological Data* (2nd ed., pp. 327-368). ISBN: 978-1-936221-48-6

Whitlock, M. C., & Schluter, D. (2015b). Designing Experiments. In *The Analysis of Biological Data* (2nd ed., pp. 423-458). ISBN: 978-1-936221-48-6

Whitsett, J. A., & Alenghat, T. (2015). Respiratory epithelial cells orchestrate pulmonary innate immunity. *Nature Immunology, 16*(1), 27-35. doi:10.1038/ni.3045

Wichmann, H. E. (2007). Diesel exhaust particles. *Inhalation Toxicology, 19*(Suppl. 1), 241-244. doi:10.1080/08958370701498075

Zachari, M. A., Chondrou, P. S., Pouliliou, S. E., Mitrakas, A. G., Abatzoglou, I., Zois, C. E., & Koukourakis, M. I. (2014). Evaluation of the alamarblue assay for adherent cell irradiation experiments. *Dose-Response, 12*(2), 246-258. doi:10.2203/dose-response.13-024.Koukourakis

Zhang, J.-M., & An, J. (2007). Cytokines, inflammation and pain. *International Anesthesiology Clinics, 45*(2), 27-37. doi:10.1097/AIA.0b013e318034194e

Øvrevik, J., Arlt, V. M., Øya, E., Nagy, E., Mollerup, S., Phillips, D. H., Låg, M., & Holme, J. A. (2010). Differential effects of nitro-PAHs and amino-PAHs on cytokine and chemokine responses in human bronchial epithelial BEAS-2B cells. *Toxicology and Applied Pharmacology, 242*(3), 270-280. doi:10.1016/j.taap.2009.10.017

Øvrevik, J., Refsnes, M., Holme, J. A., Schwarze, P. E., & Låg, M. (2013). Mechanisms of chemokine responses by polycyclic aromatic hydrocarbons in bronchial epithelial cells: Sensitization through toll-like receptor-3 priming. *Toxicology Letters, 219*(2), 125-132. doi:10.1016/j.toxlet.2013.02.014

Øvrevik, J., Refsnes, M., Låg, M., Brinchmann, B. C., Schwarze, P. E., & Holme, J. A. (2017). Triggering mechanisms and inflammatory effects of combustion exhaust particles with implication for carcinogenesis. *Basic & Clinical Pharmacology & Toxicology, 121*, 55-62. doi:10.1111/bcpt.12746

Øvrevik, J., Refsnes, M., Totlandsdal, A., Holme, J. A., Schwarze, P. E., & Låg, M. (2011). TACE/TGF-α/EGFR regulates CXCL8 in bronchial epithelial cells exposed to particulate matter components. *European Respiratory Journal, 38*(5), 1189-1199. doi:10.1183/09031936.00171110

8. Appendices

8.1. Appendix A: Results

8.1.1. Cell density differences

The importance of cell density at exposure was analyzed by looking at the CXCL8 release after 20 h exposure to pyrene as measured with sandwich ELISA. The cells were seeded at 200 000 cells/well and 400 000 cells/well and were exposed to pyrene (3, 10, and 30 μM) 20 h or 48 h after seeding, as seen in Figure 21. One experiment was conducted at each variable having two technical replicates.

Notably, exposing the cells to pyrene 20 h after seeding (Figure 21A and C) seemed to cause a more variable result compared to exposure 48 h after seeding (Figure 21B and D). The results suggest that too high of a cell density (100% confluency) may cause a variable result. Exposing two days after seeding 200 000 cells/well seemed to have the lowest variability (Figure 21B). However, these experiments are only conducted with one biological replicate, which only gives the intraexperimental variation.

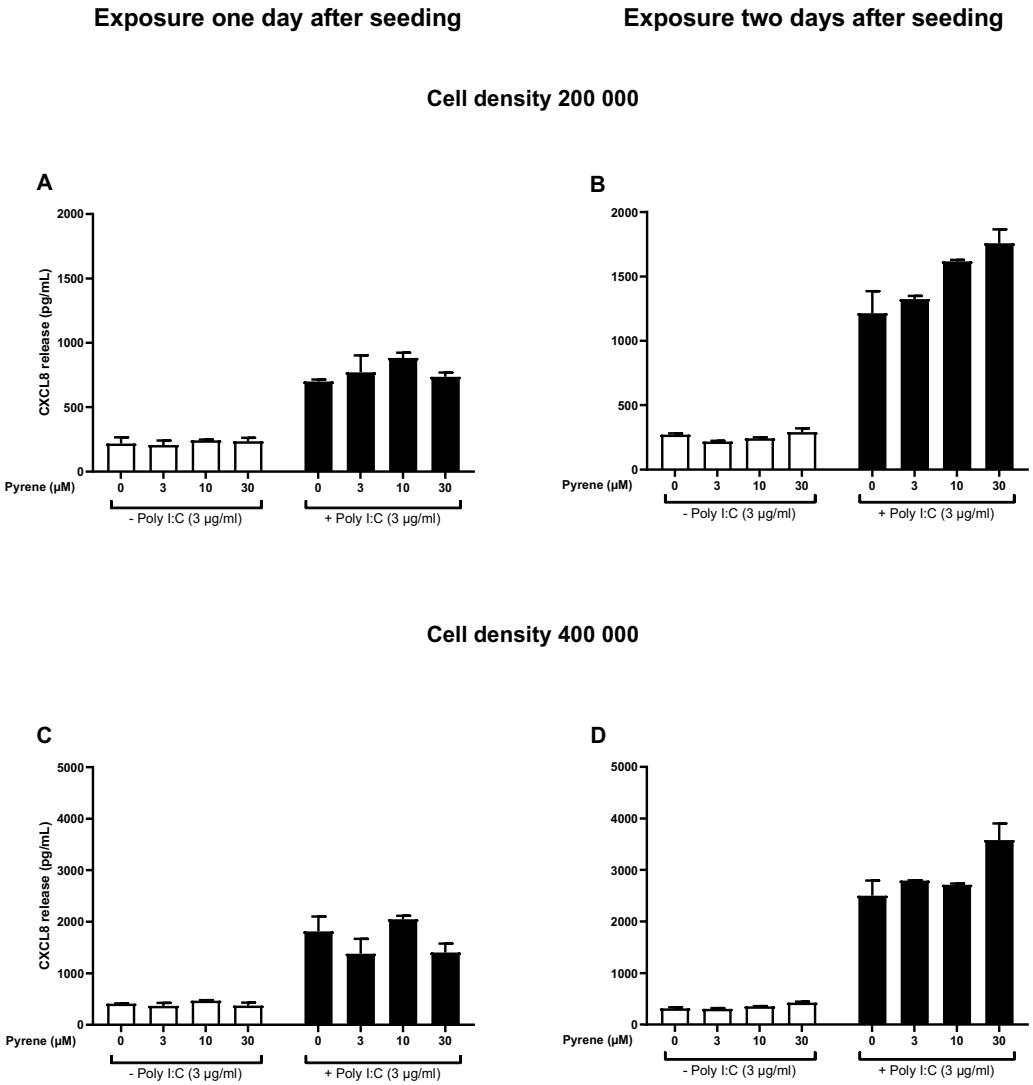

Figure 21 CXCL8 release after exposing unprimed and primed BEAS-2B cells to pyrene. *The cells were seeded with 200 000 cells/well (A and B) or 400 000 cells/well (C and D) and primed with Poly I:C (3 µg/mL) for 30 min and exposed for 20 h to pyrene (3, 10, and 30 µM), one day (A and C) or two days (B and D) after seeding. The CXCL8 release was measured using sandwich ELISA. The data are represented as the mean value ± SD of one biological replicate with two technical replicates. The results are shown as the increase in cytokine release (pg/mL).*

8.1.2. Cal-520 AM measuring pilot studies

The first experiment was conducted according to the manufacturer of Cal-520 AM (Abcam), as presented in Figure 22. In short, 20 000 cells/well were seeded in a black-wall clear-bottom 96-well plate two days before the experiment. On the day of the experiment, the medium was replaced with a new medium and a dye solution containing 5 µM Cal-520 AM, 0.04% pluronic, and 1 mM probenecid in HHBS buffer without calcium (containing (g/L): 2.0 glucose, 0.141 magnesium sulfate, 0.16 potassium phosphate monobasic, 0.35 potassium chloride, 6.9 sodium chloride). The plate was incubated with a dye solution for 90 min at 37°C and 5% CO_2 and after for 30 min at room temperature. After incubation, the dye solution was removed and replaced with an HHBS buffer containing 1 mM probenecid and the exposure stocks. Absorbance was measured at Ex/Em = 492/514 nm from time of exposure and every other minute for 120 min using Clariostar plus with 37°C incubation.

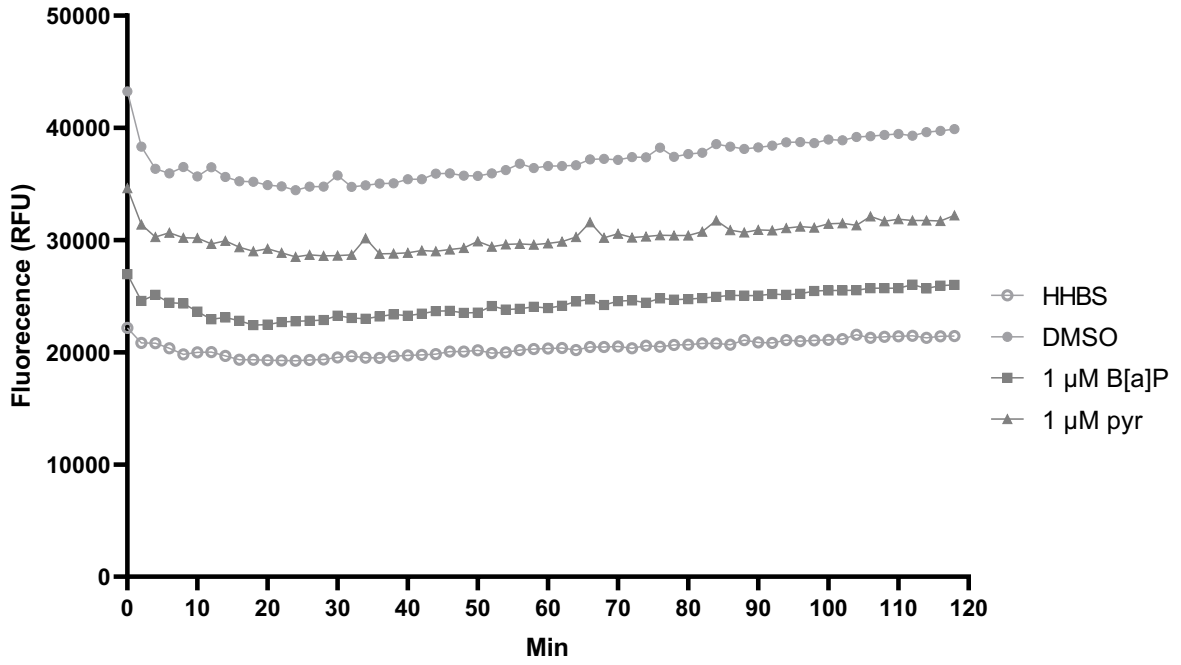

Figure 22 Fluorescence (RFU) levels after Cal-520 AM dye and exposing BEAS-2B cells to B[a]P and pyrene. *The cells were exposed to B[a]P (1 µM), and pyrene (1 µM). The Ca^{2+} levels were measured directly using Cal-520 AM. The data are represented as the mean value of one experiment with four technical replicates. The results are shown as fluorescence (RFU) increases.*

According to the first experiment (Figure 22), we hypothesized that the release of intracellular Ca^{2+} is dependent on having extracellular Ca^{2+} available. Therefore, for the second experiment (Figure 23), the HHBS buffer was changed to containing calcium (now containing (g/L): 2.0 glucose, 0.141 magnesium sulfate, 0.16 potassium phosphate monobasic, 0.35 potassium chloride, 6.9 sodium chloride, 0.373 calcium chloride, 2.1 sodium bicarbonate) and the pH was regulated to 7.2 pH before being sterilized.

The incubation time with the dye solution was reduced to 30 min at 37°C and 5% CO_2. After incubation, the dye solution was replaced with an HHBS buffer containing 2.5 mM probenecid and the exposure stocks. Measurement was conducted as described earlier.

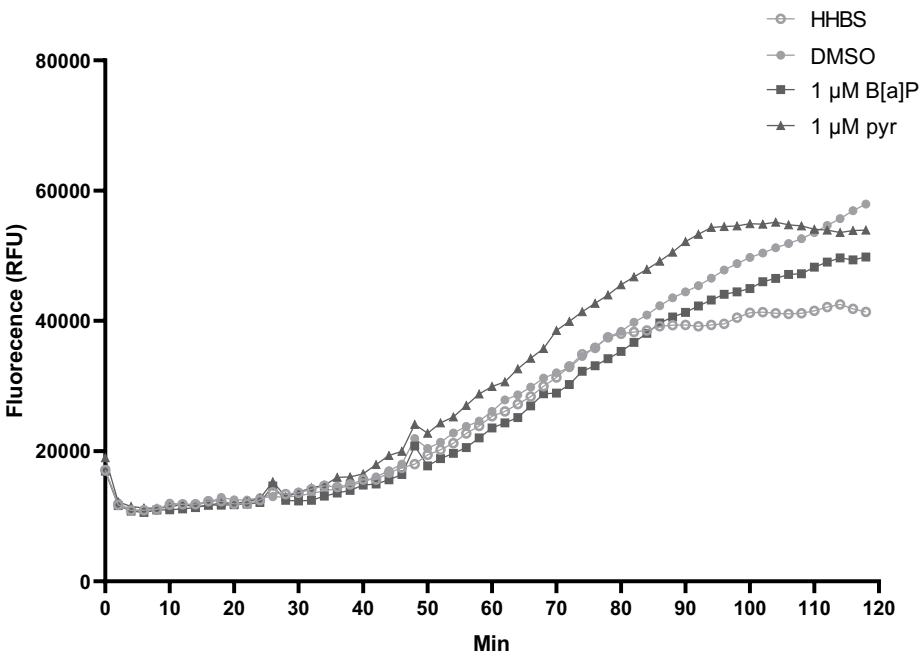

Figure 23 Fluorescence (RFU) increases after Cal-520 AM dye and exposing BEAS-2B cells to B[a]P and pyrene. *The cells were exposed to B[a]P (1 µM), and pyrene (1 µM). The Ca^{2+} levels were measured directly using Cal-520 AM. The data are represented as the mean value of one experiment with four technical replicates. The results are shown as fluorescence (RFU) increases.*

As seen in Figure 23, an increase in measured fluorescence for all exposures was seen after the second experiment, suggesting that the extracellular Ca^{2+} is essential for the intracellular release. Therefore, for the further experiments conducted, we used the same HHBS buffer and dye solution according to the second experiment.

8.2. Appendix B: Cal-520 AM Protocol

Calcium measuring using Cal-520 AM

1. 20 000 cells/well are seeded in black wall clear bottom 96 well plates
2. Cells are grown for two days without changing medium

The day of exposure:

3. Medium is removed and replaced with 100 µL new medium
4. Cells are loaded with the dye solution (see Appendix D)
5. 30 min incubation with dye solution at 37 °C and 5% CO_2
6. Dye solution are removed before adding 100 µL of HHBS buffer and 100 µL of exposure stocks
7. Measurement starts right after exposure stocks are added to the plate.
8. Calcium is measured using ClarioStar Plus with 37 °C incubation for 142 minutes

Fluorescence is measured at Ex/Em = 492/514 nm

8.3. **Appendix C: Chemicals, Reagents, and Equipment**

Cell-line	Producer
BEAS-2B	ATCC, Virginia, USA

PAHs	Producer
Pyrene	Sigma-Aldrich Norway AS
1-Nitropyrene	Sigma-Aldrich Norway AS
Phenanthrene	Sigma-Aldrich Norway AS
1-Methylphenanthrene	Santa Crus Biotechnology, Inc. Texas, USA
Fluoranthene	Sigma-Aldrich Norway AS
Benzo[*a*]pyrene	Sigma-Aldrich Norway AS
Benzo[*e*]pyrene	Sigma-Aldrich Norway AS
β-naphthoflavone	Sigma-Aldrich Norway AS

Reagents and chemicals	Producer
LHC-9 medium	Gibco, Life Technologies Corporation, California USA Grand Island, NY 14072, USA
Pure-Col coating agent	Gibco, Life Technologies Corporation, California USA Grand Island, NY 14072, USA
Pyrogen free water	Fresenius Kabi Ltd, UK
Dulbecco's Phosphate-Buffered Saline	Invitrogen, Life Technologies Ltd, UK
AlamarBlue	Invitrogen, Life Technologies Ltd, UK

BSA (albumin, bovine)	Sigma-Aldrich Norway AS
3,3',5,5'-tetramethylbenzidine (TMB)	Merck Group, Darmstadt, Germany
H_2O_2	Merck Group, Darmstadt, Germany
Tween 20	Sigma-Aldrich Norway AS
Triton-X	Sigma-Aldrich Norway AS
H_2SO_4	Merck Group, Darmstadt, Germany
NaCl	Merck Group, Darmstadt, Germany
Glucose	Sigma-Aldrich Norway AS
KCl	Merck Group, Darmstadt, Germany
Na_2PO_4	Merck Group, Darmstadt, Germany
Hepes	Sigma-Aldrich Norway AS
Trypsin	Sigma-Aldrich Norway AS
EDTA	Merck Group, Darmstadt, Germany
Sodium acetate trihydrate	Merck Group, Darmstadt, Germany
Calcium chloride dihydrate	Merck Group, Darmstadt, Germany
Sodium Bicarbonate	Merck Group, Darmstadt, Germany
1M NaOH	Merck Group, Darmstadt, Germany

Kits	**Producer**
Cytotoxicity Detection Kit (LDH) + LDH	Roche Diagnostics Deutschland, Mannheim, Germany
Cells-to-C_T 1-Step *Power* SYBR® Green Kit	Thermofisher Scientific, Massachusetts, USA

Inhibitors	Producer
CH223191	Sigma-Aldrich Norway AS

Antibodies	Producer
CXCL8 Human Antibody Pair Duoset	Invitrogen, Life Technologies Ltd, UK
IL-6 Human Antibody Pair Duoset	Invitrogen, Life Technologies Ltd, UK

Primers and reagents for Cell-to-C_T	Producer
RNase and DNase free water	Gibco, Life Technologies Corporation, California USA
Universal PCR master mix	Applied Biosystems, Life Technologies Corporation, California, USA
Lysis buffer	Applied Biosystems, Life Technologies Corporation, California, USA
DNAse and stop solution	Applied Biosystems, Life Technologies Corporation, California, USA
CYP1A1 primer	Bio-Rad Laboratories, Inc., California, USA
IL-6 primer	Integrated DNA Technologies, Inc, Iowa, USA
CXCL8 primer	Bio-Rad Laboratories, Inc., California, USA
GADPH primer	Bio-Rad Laboratories, Inc., California, USA

Immunostimulant	Producer
Poly I:C	Sigma-Aldrich Norway AS

Reagents and chemicals for Cal-520 AM	Producer
Cal-520 AM fluorophore	Abcam, Cambridge, UK
Pluronic 10%	Sigma-Aldrich Norway AS
Probenecid	Sigma-Aldrich Norway AS
Krebs-Henseleit Buffer	Sigma-Aldrich Norway AS

Equipment	Producer
TECAN Sunrise Plate Reader	TECAN Austria GmbH
7500 Fast Real-time PCR machine	Applied Biosystems, Life Technologies Corporation, California USA
ClarioStar Plus	BMG Labtech, Ramcon, Sweden
Bio-Rad CFX96 PCR machine	Bio-Rad Laboratories, Inc., California, USA
LUNA-II Automated Cell Counter	Logos Biosystems, USA

Programs	
GraphPad Prism v.8	GraphPad Software, San Diego, USA
CXF Maestro	Bio-Rad Laboratories, Inc., California, USA
Magellan 4	TECAN, Männedorf, Switzerland
MARS data analysis software V3	BMG Labtech, Ortenberg, Germany

General lab equipment	Producer
Nunc Maxisorb plate	Nunc A/S, Roskilde Denmark
Cell culture bottles	Nunc A/S, Roskilde Denmark
6-well plates	Corning, Lowell, Massachusetts, USA
96-well plates	Sarstedt A/S, Norway
Black-wall clear-bottom 96-well plates	Corning, Lowell, Massachusetts, USA

8.4. **Appendix D: Solutions and buffers**

Cell culturing

Trypsin

Trypsin	0.025 g
EDTA	0.1 g
Dulbecco's PBS	100 mL

Trypan blue

Trypan blue	0.4 g
NaCl	0.81 g
KH_2PO_4	0.06 g
Distilled water	100 mL

The solution is heated to the boiling point, cooled down, and pH adjusted to 7.2

HBS

Hepes	2.4 g
NaCl	3.5 g
KCl	0.1 g
Glucose	0.85 g
Na_2PO_4	0.97 g
Distilled water	500 mL

pH is adjusted to 7.2

Coating solution

HBS	49.5 mL
Pure Col	555 µL

Bottles and plates are incubated with the coating solution for 2 h, washed with PBS, dried, and frozen.

Solutions for sandwich ELISA

Blocking buffer

BSA	2.5 g
Dulbecco's PBS	500 mL

Diluent buffer

BSA	2.5 g
Tween 20	500 µL
Dulbecco's PBS	500 mL

Citrate buffer

Sodium acetate trihydrate	3 g
Distilled water	200 mL

pH is adjusted to 5.5 with citrate acid

TMB solution

Citrate buffer	11 mL
TMB 6 mg/mL	200 µL
H_2O_2	2.2 µL

Stop solution

H_2SO_4	50 mL
Distilled water	1000 mL

Solutions for Cell-to-C_T

Mastermix solution

Component	**In each**
Power SYBR green q-PCR	10 µL
Power SYBR green q-RT	0.16 µL
Primer (5 µM-finalt 200 nM)	1 µL
Nuclease-free water	3.84 µL
Total	**15 µL**

Solutions for Ca^{2+} measuring

HHBS buffer (Krebs)

Krebs-Henseleit buffer (1 pc.)	
Calcium chloride dihydrate	0.373 g
Sodium bicarbonate	2.1 g
Distilled water	1000

pH is adjusted to 7.2 by using 1M NaOH

25 mM Probenecid

Probenecid	72 mg
1M NaOH	300 µL
HHBS buffer	9.7 mL

Dye-solution/well

Cal-520 AM	0.50 µL
10 % pluronic	0.80 µL
25 mM probenecid	8.00 µL
HHBS buffer	90.70 µL
Total	100 µL

Exposure buffer

HHBS buffer	9 mL
25 mM probenecid	1 mL